Aerosol Science and Technology

ISSN: 0278-6826 (Print) 1521-7388 (Online) Journal homepage: http://www.tandfonline.com/loi/uast20

A review of microfluidic concepts and applications for atmospheric aerosol science

Andrew R. Metcalf, Shweta Narayan & Cari S. Dutcher

To cite this article: Andrew R. Metcalf, Shweta Narayan & Cari S. Dutcher (2018) A review of microfluidic concepts and applications for atmospheric aerosol science, Aerosol Science and Technology, 52:3, 310-329, DOI: 10.1080/02786826.2017.1408952

To link to this article: https://doi.org/10.1080/02786826.2017.1408952

AEROSOL SCIENCE AND TECHNOLOGY
2018, VOL. 52, NO. 3, 310–329
https://doi.org/10.1080/02786826.2017.1408952

A review of microfluidic concepts and applications for atmospheric aerosol science

Andrew R. Metcalf *, Shweta Narayan, and Cari S. Dutcher

Department of Mechanical Engineering, University of Minnesota, Minneapolis, Minnesota, USA

ABSTRACT

Microfluidics is used in a broad range of applications, from biology and medicine to chemistry and polymer science, because this versatile platform enables rapid and precise repeatability of measurements and experiments on a relatively low-cost laboratory platform. Despite wide-ranging uses, this powerful research platform remains under-utilized by the atmospheric aerosol science community. This review will summarize selected microfluidic concepts and tools with potential applications to aerosol science. Where appropriate, the basic operating conditions and tunable parameters in microfluidics will be compared to typical aerosol experimental methods. Microfluidics offers a number of advantages over larger-scale experiments; for example, the small volumes of sample required for experiments open a number of avenues for sample collection that are accessible to the aerosol community. Filter extraction, spot sampling, and particle-into-liquid sampling techniques could all be used to capture aerosol samples to supply microfluidic measurements and experiments. Microfluidic concepts, such as device geometries for creating emulsions and developments in particle and droplet manipulation techniques will be reviewed, and current and potential microfluidic applications to aerosol science will be discussed.

ARTICLE HISTORY
Received 27 October 2017
Accepted 10 November 2017

EDITOR
Warren Finlay

1. Introduction

Microfluidics is a large research field encompassing a number of wide-ranging disciplines, such as engineering, biology, medicine, and environmental monitoring. With miniaturization of fluid channels comes a number of key advantages available to these disciplines. The photolithography techniques used to fabricate microfluidic devices allow rapid prototyping at relatively low cost, which means that new applications for these devices can be easily explored. Short length scales (see SEM images of microchannels in Figure 1) offer practical advantages, such as smaller device footprints, making well-controlled thermal environments easier to obtain. Small devices also lead to significantly reduced volumes of sample and reagents necessary to conduct analyses, leading to lower costs and expanding the number of sample collection techniques which may be employed. More advanced fabrication techniques produce multi-layered devices that include pumps, valves, and mixing chambers on a single device (Unger et al. 2000) and temperature measurement and control alongside or embedded in fluid flow channels (Lee et al. 2017). For a more complete overview, in the online supplemental information (SI), Table S1 has a comprehensive list of microfluidic applications and review articles, SI Section 1 contains a brief history of microfluidic advances since the 1970's, and SI Section 2 has more details on fabrication techniques and materials used in microfluidics. In general, these all-in-one microfluidic devices can include sample injection, movement, mixing, reaction, separation, and detection and are appropriately called a "lab-on-a-chip" (Stone et al. 2004; Whitesides 2006).

Aerosol science can also tap into the benefits of using a microfluidic platform. Biphasic (droplet) microfluidics can be used to (1) study interfacial phenomena of aerosol chemical mimics using droplets (liquid–liquid interface) or bubbles (liquid–air interface) and (2) encapsulate an aerosol particle in one phase (e.g., an aqueous phase for dissolution of water-soluble species) for transport by an immiscible, carrier phase. Once in the device, rapid sorting, manipulation, and measurements are possible with a variety of geometries. Already, recent studies have begun

CONTACT Cari S. Dutcher cdutcher@umn.edu Department of Mechanical Engineering, University of Minnesota, 11 Church St. SE, Minneapolis, MN 55455, USA.

*Current affiliation: Department of Environmental Engineering and Earth Sciences, Clemson University, Anderson, South Carolina, USA

Color versions of one or more of the figures in the article can be found online at www.tandfonline.com/uast.

Supplemental data for this article can be accessed on the publisher's website.

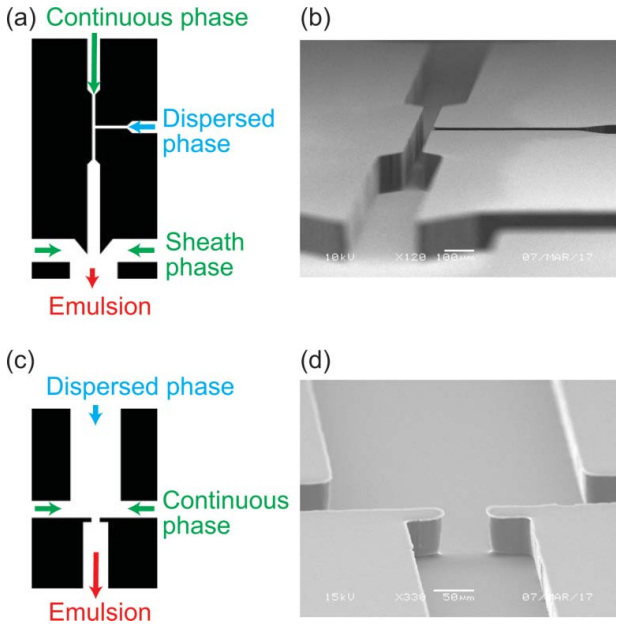

Figure 1. Microfluidic channel masks (left) and SEM images of the corresponding PDMS channels (right) of a T-junction (top) and co-flow with flow focusing (bottom) geometries. In the mask images (left), arrows denoting continuous, dispersed, sheath, and emulsion flows show direction of flow and approximate relative velocities (proportional to arrow length) of the flow in each channel.

to use microfluidics for measurements of interfacial tension to characterize chemical mimics of atmospheric aerosol (Metcalf et al. 2016; Boyer and Dutcher 2017) and for detection of bioaerosol hazards (Damit 2017). In recent development of low-cost sensors, microfluidic and micro electromechanical systems (MEMS) devices have seen increasing application, such as the air-microfluidics based PM 2.5 sensor that can be used for affordable personal monitoring of hazards such as tobacco smoke or diesel exhaust (Paprotny et al. 2013). In addition, a microfluidic nebulizer could improve the monodispersity of aerosol populations for calibration of traditional aerosol sampling instruments (Amstad et al. 2017).

This review will describe selected microfluidic concepts from the perspective of atmospheric aerosol science. Where appropriate, current applications of microfluidics to aerosol science will be reviewed, and potential applications will be presented. Section 2 will discuss basic microfluidic flow concepts with comparisons to typical atmospheric aerosol analogues. A review of selected microfluidic experimental capabilities, including control by electrical, chemical, and temperature gradients, will demonstrate the versatility of the microfluidic platform. Section 3 will discuss using microfluidics as a measurement platform to characterize physical, chemical, and thermodynamic properties of fluids relevant to atmospheric aerosol science. Section 4 will discuss microfluidic experiments which can be used to observe specific phenomena which occur in atmospheric aerosol and will draw comparisons to single-particle techniques currently employed by the aerosol community. In each section, the similarities and differences between the microfluidic framework and traditional atmospheric aerosol science will be discussed.

2. Microscale phenomena

2.1. Dimensionless groups in microfluidic flow and aerosol science

Several key dimensionless groups for single-phase and two-phase microfluidic flows are detailed below and compared to analogs in atmospheric and laboratory aerosol studies. One hallmark characteristic of microfluidic flow is that viscous forces dominate over inertial forces, resulting in laminar flow. This flow type can be described using the Reynolds number, *Re*, the ratio of inertial to viscous forces, and is most generally expressed as

$$Re = \frac{Ul}{\nu} \quad [1]$$

where U is characteristic fluid velocity, l is characteristic object length, and ν is fluid kinematic viscosity. In a microfluidic device with a rectangular channel cross-section, U is typically the average velocity of fluid flow in the channel and l is the hydraulic diameter of the flow channel (Gravesen et al. 1993; Christopher and Anna 2007). Typical channel dimensions and flow rates used in microfluidic devices lead to $Re \ll 1$, which is laminar flow (Purcell 1977). Atmospheric aerosol scientists typically consider *Re* from two perspectives. The first is for the flow of particle-laden air in a sampling tube of an instrument, which is typically desired to be laminar flow ($Re < 2000$) to reduce the amount of particle losses due to inertial deposition onto the tubing walls. The second perspective is for particle Reynolds number, Re_p, in which flow is considered laminar for $Re_p < \sim 0.1$ (Kulkarni et al. 2011). In a channel, *Re* characterizes whether fluid flow is turbulent or laminar and a similarity in *Re* means a similarity in flow kinematics (Hinds 1999).

Figure 2 displays a comparison of flow regimes over a range of microfluidic and aerosol particle sampling conditions. The key difference between the microfluidic framework and the aerosol sampling regime in Figure 2 is that microfluidics usually involves the flow of liquid and aerosol sampling involves the flow of particle-laden air. The orders of magnitude difference in viscosity and typically faster flow velocities in aerosol sampling lead to a significantly smaller *Re* in typical microfluidic experi-

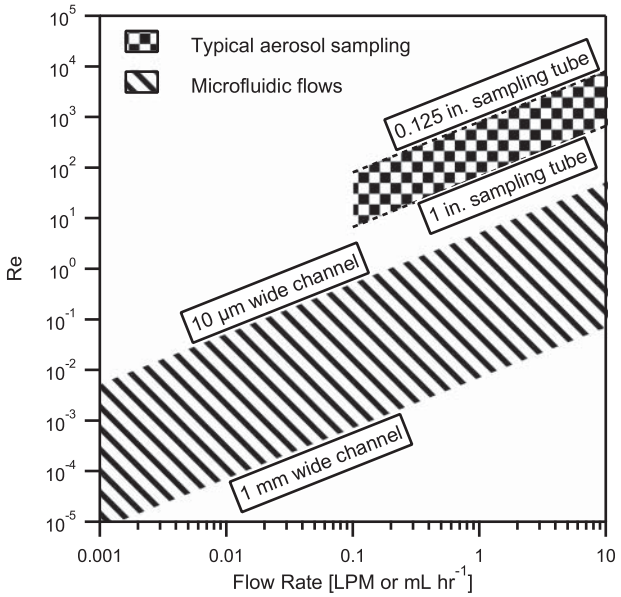

Figure 2. Relevant flow regimes in microfluidic flows (use mL hr^{-1}) and typical aerosol particle sampling (use liters per minute, LPM), for a given volumetric flow rate at a fixed hydraulic diameter. Microfluidic flow is considered in channels 100 μm tall ranging from 10 μm wide with ethanol ($\nu = 0.983$ cSt) to 1 mm wide with heavy mineral oil ($\nu = 70$ cSt). Typical microfluidic flows have Re < 1. Typical aerosol particle sampling is considered for sample tubing from about 1/8 in. to 1 in. diameter for sampling particles in air ($\eta = 18.2$ μPa s).

ments as compared to aerosol particle sampling conditions. Both flows are typically laminar, and microfluidics provides a wider range of typical operating conditions well below the critical Reynolds number.

While single-phase microfluidics may prove useful for some applications, the use of two or more immiscible fluid phases greatly expands the number of applications available to microfluidics. The observed physics accessible in multi-phase microfluidics is typically described by several dimensionless groups (e.g., Squires and Quake 2005). Note that the dimensionless groups are organized according to their dominant use but may be relevant for other applications than those discussed here. To compare flow regimes between typical microfluidic and aerosol applications, "model" microfluidic channels and aerosol particles are considered. The model microfluidic channel is a straight 200 μm wide by 100 μm tall channel with 1 μL min^{-1} flow of silicone oil (poly(dimethylsiloxane), $\rho = 0.96\ g\ mL^{-1}$, $\eta = 45\ mPa\ s$, Fisher Scientific, CAS 63148-62-9) (Barca et al. 2014). The model aerosol particle is 1 μm diameter and $\rho_p = 1.58\ g\ cm^{-3}$ (Cross et al. 2007) in "Normal Air" (NTP, $p = 1\ atm$, $T = 293\ K$) (Kulkarni et al. 2011).

In multiphase flows, it is important to distinguish between continuum flow, in which the discrete molecular nature of a carrier fluid is ignored, and slip flow, in which a dispersed phase (usually solid or liquid particles) can "slip" between the fluid molecules of the carrier phase. To describe the flow regime, the Knudsen number, *Kn*,

$$Kn = \frac{\lambda}{l} \quad [2]$$

is defined as the ratio of the material dimension, λ, which depends on the fluid, to the characteristic flow dimension, l, through or around which the fluid is traveling. The material dimension is the mean free path (gases), molecular spacing (liquids), or grain size (solids). The characteristic length scale is particle diameter, when describing particle-laden flow, or channel dimension (usually hydraulic diameter), when describing microfluidic flow. Typically, $Kn < 1$ defines continuum flow, $Kn \gg 1$ defines free molecular or kinetic flow, and *Kn* between these extremes defines the transition regime (Squires and Quake 2005; Kulkarni et al. 2011; Seinfeld and Pandis 2016). In both microfluidics and aerosol science, the characteristic length scales can be on the same order as the material dimension leading to a range of possible flow regimes. For gas flows especially, several flow regimes can occur within the same microchannel (Gad-el-Hak 1999). In the design of microfluidic experiments, *Kn* can be tuned to define a flow field which mimics an aerosol flow of interest.

Because the flow inside microfluidic devices is laminar and slow, either advection or diffusion or both may play a role in the mixing of immiscible fluids. The Péclet number (Pé) is a dimensionless number which compares the relative effects of advective to diffusive transport,

$$Pé = \frac{Ul}{D} \quad [3]$$

where U is the fluid velocity, l is the characteristic length scale (of a boundary towards which diffusion is occurring), and D is the diffusivity (of molecules or particles in the fluid flow). Depending on the exact experimental setup, Pé can be defined in a number of ways. For typical straight microfluidic channels >100 μm wide, *Pé* is large, indicating that advection of the fluid contents downstream is more important than diffusion to the walls of the flow channel. Geometries can also be designed to explore low and moderate *Pé* regimes to control diffusional mixing of two parallel-flowing fluids (Alvarez et al. 2012).

In some microfluidic experiments, the diffusion of molecules to a trapped bubble, droplet, or solid particle is of interest, in which case l is the particle diameter. In these examples, the diffusivity is for whatever component in the carrier fluid is of interest, whether it be surfactant molecules or bubbles, droplets, or solid particles carried

by the flow. In aerosol science, the Péclet number is often used to describe filter efficiency, where l is the width of a single fiber of the filter and D is the particle diffusion coefficient given by the Stokes–Einstein equation (Hinds 1999). Other forms of the Péclet number are used to describe particle migration and penetration efficiencies through devices (Kulkarni et al. 2011). In either application (microfluidics or aerosol), a large Péclet number indicates that advective transport processes are dominant, whereas a small Péclet number indicates that diffusion processes are dominant. Both applications can access similar advection- or diffusion-dominated flow regimes.

Surfaces and interfaces in biphasic microfluidic flows are important and dictate a number of physical processes. As the characteristic length decreases in the transition from macro- to micro-scale biphasic flows, the interface-to-volume ratio increases. Therefore, as an experiment is scaled down to the microscale, interfacial forces, such as interfacial tension gradients and shear stresses, become dominant over volume forces, such as gravity and inertia (Bruus 2011). Consequently, one has to consider the effect of interfacial tension, capillary, and Marangoni forces, typically expressed as dimensionless groups such as Capillary number (*Ca*), Bond number (*Bo*), and Weber number (*We*) to understand the flow regimes typically encountered in microfluidic devices. While not widely used in atmospheric aerosol science, these dimensionless numbers are important for understanding and operating microfluidic devices, and so are included here.

The Capillary number *Ca* is the ratio of viscous forces to interfacial tension,

$$Ca = \frac{U\eta}{\gamma} \quad [4]$$

where η is the dynamic viscosity and γ is the interfacial tension. Microfluidic flow driven by syringe pumps can typically access Capillary numbers ranging from $\sim 10^{-3}$ to 10^{1}, meaning that a range of interface formation regimes are possible (Christopher and Anna 2007). For comparison, for flow of air at 5–20 mph around a water droplet with surface tension of 72 mN m^{-1}, the Capillary number ranges from 10^{-4}–10^{-3}. Because the viscosity of air is small, interfacial forces typically dominate viscous forces on particles in the atmosphere. However, the presence of surfactants in atmospheric aerosol particles has the potential to dramatically lower interfacial (surface) tension of liquid particles which would raise atmospheric *Ca* (Petters and Petters 2016).

The Bond number (*Bo*) is the ratio of gravitational forces (hydrostatic pressure) to interfacial tension and is a metric for the relative importance of body forces to surface forces in fluid flows. The Bond number is used to analyze the shape distortion of droplets in a continuous medium, such as in pendant drop experiments to measure interfacial tension (Berry et al. 2015), and is defined as

$$Bo = \frac{\Delta\rho g h^2}{\gamma} \quad [5]$$

where $\Delta\rho$ is the difference in densities between the two phases, h is the characteristic length, and γ is the interfacial tension between fluid phases. In a pendant drop measurement, interfacial tension holds a microscale droplet opposed by gravity on the tip of a capillary; measurement of this force balance is what allows determination of interfacial tension. On the microscale, because interfacial forces have a much greater influence on the system as compared to gravity, the droplets do not fall off the capillary and *Bo* is typically much less than unity. *Bo* is commonly on the order of 10^{-3} for both horizontal and vertical orientations of a typical microfluidic device (Takeuchi et al. 2005). In the atmosphere, *Bo* would be similarly small owing to smaller droplets and potentially higher surface tensions; however, aerosol scientists rarely consider cases in which aerosol particles are "clinging" to another object.

Finally, the Weber number (*We*), is the ratio of inertial forces to interfacial tension and is defined as the product of the Reynolds and Capillary numbers,

$$We = Re * Ca = \frac{U^2 l\rho}{\gamma} \quad [6]$$

The Weber number is significant when inertia and capillary forces are greater than the viscous stresses, but this is not often the case for either aerosol or microfluidic applications, which both have typical Weber number values in the range of 10^{-5}–10^{-2}. The exception is for dynamic events such as bubble formation and droplet break-up, where both inertial and viscous forces could have a pronounced effect on the process even though the flow remains laminar (Garstecki et al. 2005; Zhao et al. 2006; Christopher and Anna 2007).

2.2. Droplet generation

When considering two-phase microfluidic flows, droplet microfluidics is potentially applicable to aerosol science in two key ways: (1) to study the interfacial properties of aerosol chemical mimics and (2) to encapsulate an aerosol particle for transport and manipulation. Shearing one immiscible fluid by another forms droplets by competition between two primary stresses: viscous stresses which deform the fluid interface and capillary stresses which resist deformation (Taylor 1934; Christopher and Anna

2007). The microchannel geometry plays an integral role in determining the type of flow field, which in turn controls the nature of fluid shearing. There are several categories of geometries that are used to generate droplets or bubbles in microfluidic devices (see Figure 1 and Figure S2), and these are discussed in detail in Section 4 of the SI. The fluids' viscosities, densities, and interfacial tension also influence the droplet formation process. Figure S2 displays images of drop generation from these different geometries. Figure S3 shows droplet size as a function of flow parameters for two droplet/bubble formation regimes in a T-junction geometry. Figure S3 demonstrates both the predictability of droplet size and the tenability of microfluidic devices for droplet generation.

In comparison to most classical aerosol generation techniques, microfluidic droplet-generation techniques offer a distinct advantage in the ability to produce highly monodisperse droplets, primarily owing to the confined microchannel geometry (Anna 2016). Unconfined geometries, found in, for example, electrosprays, nebulizers, atomizers, and vibrating orifice aerosol generators (VOAGs), lead to a higher degree of polydispersity of the generated aerosol population (see Table 1 for a review of typical operating parameters for these aerosol generation sources). The polydispersity of droplets in a population is quantified by the coefficient of variation (α, in units of percent),

$$\alpha = \frac{\sigma_{D_p}}{\overline{D}_p} \times 100 \qquad [7]$$

where σ_{D_p} is the standard deviation on diameter of the size distribution of the emulsed droplets and $\overline{D}_p$ is the number-weighted mean diameter. The polydispersity of emulsed droplets from early "T-junction" microchannel array devices were less than 2% (Kobayashi et al. 1999), which was an immediate improvement over traditional emulsification techniques which typically produced a polydispersity of 10% or more (Sugiura et al. 2001b). With few exceptions, most traditional aerosol generation methods have a much larger polydispersity than microfluidic methods (Table 1). Polydisperse aerosol generation methods require the use of an aerosol classifier, such as a differential mobility analyzer (DMA), to generate a monodisperse aerosol population; but even then, multiple charging of aerosol particles can introduce artifacts from larger particles.

Table 2 compares typical particle diameters among biphasic microfluidics, single-particle aerosol experiments, traditional aerosol sampling instruments, and typical atmospheric classification of aerosol sizes. Clearly, microfluidics already operates in sizes similar to large coarse mode aerosol particles and cloud droplets. One potential limitation of current droplet microfluidics is that generated droplet sizes are typically larger than fine and ultrafine aerosol particles typically sampled in the atmosphere. Access to smaller droplet diameters, in the range of several hundred nanometers, is possible in some microfluidic geometries, and further emphasis on small-droplet techniques will broaden applications to aerosol science (Anna et al. 2003).

Beyond simple two-phase flows, microfluidics can also be used to precisely fabricate "designer emulsions" in a stable and repeatable manner (Shah et al. 2008). "Designer emulsions" simply refers to an emulsion in which the droplets have a complex morphology. These

Table 1. Selected aerosol generation techniques with typical size distribution parameters. CV is coefficient of variance, α, (Equation (7)).

Aerosol generation method	Median Diameter [μm]	CV [%]	Reference
Laboratory techniques			
Capillary aerosol generator (CAG)	0.29–3.40[1]	30–100	(Gupta et al. 2003)
Modified Collison atomizer	0.032–1.3[2]	18–35	(Liu and Lee 1975)
DeVilbis nebulizer	2.8–4.2	80–90	(Hinds 1999)
Lovelace nebulizer	2.6–5.8	80–130	(Hinds 1999)
Vibrating orifice monodisperse aerosol generator (VOAG)	0.5–50[3]	~1.4	(Berglund and Liu 1973)
Electrohydrodynamic (EHD) atomization	~10–2,000	–[4]	(Cloupeau and Prunet-Foch 1994; Grace and Marijnissen 1994)
Sintered glass filter	60 nm	–[4]	(Prather et al. 2013)
Piezo-activated drop-on-demand generator	10–100	<1	(Ulmke et al. 2001; Vaughn et al. 2016)
Piezoceramic dispenser/droplet chain technique	0.3–18	–[4]	(Baldelli et al. 2016)
Microfluidic techniques			
Microchannel emulsification	~20	<2	(Kobayashi et al. 1999; Kawakatsu et al. 2001)
T-junction	~30–200	<2	(Garstecki et al. 2006; Christopher et al. 2008)
Co-flow	20–200	<2	(Nisisako et al. 2006)
Flow-focusing	<1–600	<1	(Anna et al. 2003; Seo et al. 2007)
Microfluidic spray dryer[5]	40 nm	–[4]	(Thiele et al. 2011)
Microfluidic nebulator[5]	14; 300 nm	–[4]	(Amstad et al. 2015; 2017)

[1]Aerodynamic diameter; [2]mobility diameter; [3]physical diameter; [4]no data given; [5]generates liquid droplets in air.

Table 2. Comparison of typical particle diameters for various aerosol experiment setups, sampling instruments, and atmospheric conditions. Although biphasic microfluidics is typically operated at droplet sizes at the large end of coarse mode aerosol and into the cloud droplet regime, more refinement of microfluidic droplet generation techniques will lower the smallest diameters accessible to microfluidic experiments.

Experimental framework	Particle diameter	Reference
Biphasic microfluidics	~30–200 μm	*this study*, (Metcalf et al. 2016)
Electrodynamic Balance (EDB)	2–20 μm	(Colberg et al. 2004)
	6–40 μm	(Davis et al. 1990)
	14–44 μm	(Davies et al. 2012)
	20–65 μm	(Song et al. 2013)
	~20–50 μm	(Pope et al. 2010)
	40–80 μm	(Steiner et al. 1999)
	100–250 μm	(Davis 1997)
Optical tweezers	0.025–10 μm	(Ashkin et al. 1986)
	1–10 μm	(Mitchem and Reid 2008)
	5–10 μm	(Bzdek et al. 2016)
Acoustic levitation	10 μm–5 mm	(Trinh 1985; Warschat and Riedel 2017)
Aerosol sampling instruments		
Nanometer Differential Mobility Analyzer (Nano-DMA)	3–50 nm	(Chen et al. 1998)
Radial Differential Mobility Analyzer (RDMA)	3–200 nm	(Zhang et al. 1995)
Differential Mobility Analyzer (DMA)	5 nm–1 μm	(Knutson and Whitby 1975)
Electrical aerosol analyzer	6 nm–1 μm	(Liu and Pui 1975)
Aerodynamic lens	20–240 nm	(Liu et al. 1995)
Aerosol Particle Mass Analyzer (APM)	~20–700 nm	(Ehara et al. 1996)
Couette Centrifugal Particle Mass Analyzer (CPMA)	50 – ~600 nm	(Olfert et al. 2006)
Particle bounce measurements in cascade impactor	30–120 nm	(Virtanen et al. 2010)
Wide-range Particle Spectrometer	0.01–10 μm	(Liu et al. 2010)
Aerodynamic Particle Sizer (APS)	0.5–16 μm	(Chen et al. 2007)
Atmospheric conditions		(Hinds 1999; Pruppacher and Klett 2004; Seinfeld and Pandis 2016)
Nucleation mode (ultrafine particles)	<10 nm	
Aitken mode (ultrafine particles)	10–100 nm	
Accumulation mode (fine particles)	0.1–2 μm	
Coarse mode (coarse particles)	2–50 μm	
Cloud droplet	5–100 μm	
Rain drop	0.05–10 mm	

morphologies include core-shell particles, also called "double emulsions" because it is a droplet inside a droplet, and "multiple emulsions," so called because many immiscible layers can be stacked within a single droplet (Utada et al. 2005, 2007; Chu et al. 2007b; Abate and Weitz 2009). Multiple emulsions are commonly formed by stacking single-emulsion geometries in series, meaning that although the droplet morphologies are complex, the microfluidic methods to produce these droplets are not significantly more complex than single-droplet generation methods (Okushima et al. 2004; Utada et al. 2007). Many other possible particle morphologies can be fabricated with these techniques, including solid particles, porous particles, vesicles, colloidal gel particles, and liquid crystal shells (Sugiura et al. 2001a, 2002; Hayward et al. 2006; Fernández-Nieves et al. 2007; Kim et al. 2007; Chu et al. 2007a; Dubinsky et al. 2008; Wan et al. 2008; Duncanson et al. 2012). Many of these morphologies, especially core-shell and multiphase particles, are hypothesized to occur naturally in atmospheric aerosol particles (Freedman et al. 2010; Freney et al. 2010; You et al. 2012), meaning that generation of these particle types in a microfluidic device with the proper chemical mimics could provide a powerful tool for aerosol experimentation.

2.3. Microfluidic controls and external fields

Microfluidic devices are versatile with a wide range of bubble, droplet, and particle manipulation and measurement methods available. Many of these methods allow noninvasive, noncontact experiments on neutral, charged, magnetic, photophoretic, and chemically mobile particles that are of potential importance to aerosol science. A number of experimental controls are available to microfluidics, and their small size usually leads to improved control as compared to larger-scale experiments. Microfluidic flows can be driven by forces both internal and external to devices (Stone et al. 2004). One of the most common methods to drive flow in these devices is with syringe pumps that supply a constant volumetric flow rate (Figure S1A). Some limitations from using syringe pumps, including slower flow equilibration times, are discussed in Section 3 of the SI. An alternative to using syringe pumps is air-pressure-driven flows

(Figure S1B), where compressed air is supplied to a reservoir of liquid which is connected to the microfluidic device by rigid tubing (Bong et al. 2011). Flow calibration relating air pressure to volumetric flow rates are easily obtained, and computer-controlled pressure regulators allow automated flow control during an experiment.

Because of the small size of microfluidic devices, thermal equilibrium driven by a temperature-controlled microscope stage is possible. Recent studies use microfluidic devices to generate water droplets which are then collected in a trap array and transferred to a cryostage to observe freezing events which characterize the presence of ice nuclei particles within those droplets (Riechers et al. 2013; Reicher et al. 2017). A multi-zone, custom-built cold stage (see Figure 3a) has been used to homogeneously freeze water droplets near −40°C (Stan et al. 2009). Thermoelectric temperature control devices, such as Peltier elements, can be conveniently incorporated into multi-layer lab-on-a-chip devices (Erickson and Li 2004). An embedded electric heater can induce surface tension gradients which precisely control the size of daughter droplets formed during parent droplet breakup in a bifurcated channel (Ting et al. 2006). Temperature-dependent interfacial tension measurements based on droplet deformation have been performed by integrating microheaters into a conventional contraction-expansion device (Lee et al. 2017). Temperature-induced surface tension gradients can also be generated using lasers, and the resulting thermo-capillary effects can be harnessed to block droplet motion, leading to merging of droplets (Baroud et al. 2007).

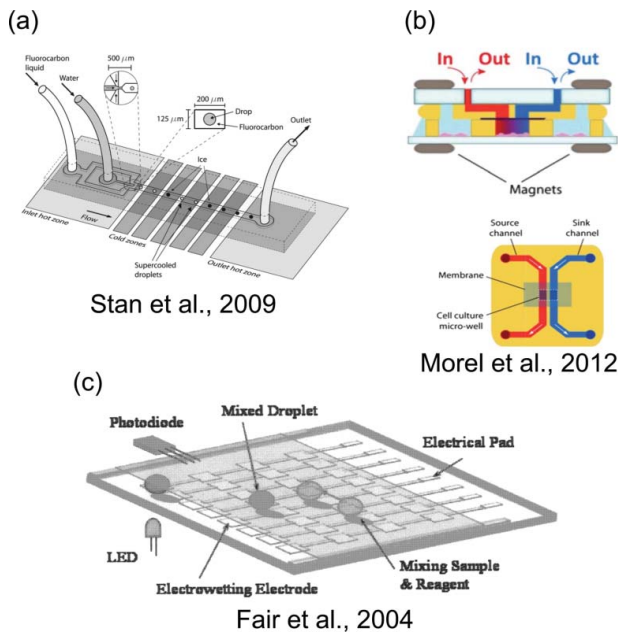

Figure 3. Selected microfluidic methods for producing temperature gradients, chemical gradients, and electric fields. (a) Reproduced from Stan, C. A., Schneider, G. F., Shevkoplyas, S. S., Hashimoto, M., Ibanescu, M., Wiley, B. J. and Whitesides, G. M. (2009). A Microfluidic Apparatus for the Study of Ice Nucleation in Supercooled Water Drops. *Lab Chip*, 9(16):2293–2305 with permission of The Royal Society of Chemistry. (b) Reproduced from Morel, M., Galas, J.-C., Dahan, M. and Studer, V. (2012). Concentration Landscape Generators for Shear Free Dynamic Chemical Stimulation. *Lab Chip*, 12(7):1340–1346 with permission of The Royal Society of Chemistry. (c) Reproduced from Fair, R. B., Khlystov, A., Srinivasan, V., Pamula, V. K. and Weaver, K. N. (2004). Integrated Chemical/Biochemical Sample Collection, Pre-Concentration, and Analysis on a Digital Microfluidic Lab-on-a-Chip Platform. Edited by Linda A Smith and Daniel Sobek. *Proc. SPIE*, 5591:113–124 with permission of SPIE.

Chemical gradients are also possible in microfluidic devices, which serve as viable platforms to recreate and study cellular systems *in vitro* (Zhang et al. 2015; Shamloo and Amirifar 2016). The motion of cells in response to the release of certain bio-chemicals leads to the phenomenon called chemotaxis, and such motion is dominated by diffusion ($Pé < 1$) due to chemical gradients rather than flow-induced advection. Micro-tunnels interlinking two main flow channels in a microfluidic chip create a chemical gradient parallel to the direction of flow, inducing chemotaxis (Li et al. 2007). Flow-focusing in a microfluidic device containing a membrane (see Figure 3b) can create concentration gradients for cell-based assays in a shear-free environment (Morel et al. 2012). Conversely, convection-based gradients can be generated in a microfluidic channel ($Pé > 1$). These designs have been used in biological applications to study the behavior of cells in dynamic flow-dominated environments (Toh et al. 2014). Additionally, chemical gradients can be created by employing a so-called 'Christmas tree design' which incorporates multiple serpentine mixing channels in a pyramid-shaped arrangement and has primarily been used to study the chemotaxis of cells in the presence of diverse, time-varying chemical gradients (Jeon et al. 2002). Use of chemical gradients may find applications in studies of biological aerosol particles and their response to different environments.

Electric fields applied to microchannels sort particles by the implementation of two distinct physical mechanisms, namely, electrophoresis and dielectrophoresis (Zhu and Xuan 2009). While electrophoretic techniques are effective for particles containing charged species, dielectrophoresis is exhibited by neutral particles subjected to a nonuniform electric field (Rahman et al. 2017). Dielectrophoresis using microelectrodes placed beneath a PDMS channel has been employed to achieve rapid sorting of droplets and particles (Ahn et al. 2006). Forces greater than 10 nN were produced on a water droplet and sorting rates in excess of 1.6 kHz were achieved using this setup. Electrophoresis, while also traditionally applied in applications involving particle or cell sorting (Shields et al. 2015),

can be applied to perform measurements of fundamental properties such as electrophoretic mobility and zeta potential (Karam et al. 2017).

Picoliter to microliter-sized droplets placed in contact with a conducting substrate can be manipulated using electric or magnetic fields, using a microfluidic platform called 'digital microfluidics' (DMF). DMF systems typically constitute an array of electrodes coated with insulating and hydrophobic materials, such as Teflon-AF, on which droplets are manipulated (Abdelgawad and Wheeler 2009). DMF employs electro-wetting to manipulate discrete drops by harnessing the gradients in interfacial energy caused by applying a voltage across the electrode array (Welters and Fokkink 1998). One difference between digital systems and conventional microfluidic systems is the absence of channels, pumps, or valves, which are not required for digital systems. Another difference is that digital systems can be used to manipulate each droplet to perform trapping, merging, splitting, or transport operations independent of others, whereas a conventional microfluidic device carries out these same operations on a series of droplets. Additionally, digital systems allow droplets to be exposed to air, without necessarily having to be confined in an outer immiscible fluid, to accommodate carrying out operations such as evaporation of droplets. However, if the intent is to avoid evaporation, droplets can either be encapsulated in an oil film (Fair et al. 2004), or immersed in an immiscible oil phase between a top plate (ground electrode) and bottom plate containing the active electrode array (Fair et al. 2007). DMF platforms integrated with conventional microfluidic platforms are also gaining popularity, because sample collection, reagent mixing, and transport can be easily performed in a DMF device, followed by sorting and other high-throughput operations in a micro-channel device (Jebrail et al. 2012).

Digital microfluidic platforms have been employed for aerosol particle sampling and analyte detection. One study combines a conventional impactor with a DMF device to achieve rapid detection of inorganics such as sulfates in aerosols (Fair et al. 2004, 2007). In this work (see Figure 3c), a stream of aerosol particles is directed towards a section of the digital microfluidic chip containing electrodes on the bottom surface. After impaction of the aerosol, a microliter droplet is manipulated using electrowetting to collect the aerosol particles as the droplet is transported across the surface (also called the washing stage). Thereafter, the droplet is treated with reagents to measure the concentrations of analytes present in the sample with the aid of on-chip LEDs and photo detectors. The DMF impactor device can also encapsulate the droplet in an oil film to arrest evaporation (Fair et al. 2004) and to perform the remaining operations (detection of analytes) using two-plate electrodes with silicone oil between the plates (Fair et al. 2007). The DMF method of sample collection and detection has sampling intervals as short as 1 min, which is a significant improvement over conventional filter sampling techniques which require longer sampling intervals and manual extraction of the filters. Moreover, the sample collected by the scanning droplet is more highly concentrated because the DMF method consumes extremely small volumes of reagent.

DMF devices can also be employed for sample preparation for mass spectrometry, to achieve off-line as well as in-line analysis of samples (Kirby and Wheeler 2013). For example, dried blood spot samples preserved on a filter paper medium were extracted using solvent droplets on a digital microfluidic chip and then analyzed using Nano-electrospray Ionization Mass Spectrometry (Jebrail et al. 2011). In-line analysis can be facilitated by using capillary or microchannel emitters which introduce the sample directly from the DMF device to the mass spectrometer, without manual handling of the samples (Jebrail et al. 2011; Shih et al. 2012; Kirby and Wheeler 2013).

The flow concepts and microfluidic controls presented here can be used in a variety of applications relevant for aerosol scientists. The next two sections of this review present a number of potential applications and are organized as follows. First, using microfluidics for chemical and physical measurements is discussed in Section 3. In this application, microfluidic devices are the instruments on which these measurements are made and the goal of the measurement is to characterize the properties and behavior of the dispersed phase. Second, in Section 4, using microfluidics to mimic physical phenomena as a complement to traditional single particle methods is discussed. In this application, microfluidic devices are the platform on which experiments are performed to mimic phenomena which occur in atmospheric aerosol particles.

3. Chemical and physical measurements

In laboratory studies aimed at understanding fundamental chemical and physical mechanisms found in atmospheric aerosol particles, chemical mimics are often used as key surrogates for ambient particles. In environmental chambers, inorganic electrolytes are often used as seed particles for secondary aerosol growth during experiments (Cocker et al. 2001). Biogenic salts are also an important aerosol seed in the atmosphere (Pöhlker et al. 2012). The chemical mechanisms which lead to secondary organic aerosol formation from gas-phase precursors are often studied and characterized with lab-synthesized intermediate chemicals (Lin et al. 2012; Zhang et al. 2012; Kramer et al. 2016). Heterogeneous chemistry which occurs in ambient aerosol particles is also

mimicked in laboratory beakers to understand how chemical processing proceeds in the atmosphere (Shapiro et al. 2009; Sareen et al. 2010; Schwier et al. 2010; Li et al. 2011; Schwier et al. 2012, 2013). Microfluidics may be employed for these studies and has some advantages over traditional bulk techniques; notably that required sample volumes are typically much smaller and yet many repeat measurements may be made. This section highlights a few applications in which microfluidics can be used for chemical and physical measurements of aerosol chemical mimics.

3.1. Interfacial measurements

Surfaces of aerosol particles can constitute a significant driving force behind atmospheric phenomena such as ice and cloud condensation, evaporation and condensation kinetics, and particle morphology (Bertram et al. 2001; Folkers et al. 2003; McNeill et al. 2006; George and Abbatt 2010; Baustian et al. 2012; Davies et al. 2013). Surface tension, σ, the molecular tension at the interface between a solid or liquid phase and a gas, results from unbalanced intermolecular attraction which causes surfaces to contract spontaneously to minimize the surface area, or free energy of the interface (Davies and Rideal 1963). The surface tension of liquid aerosol particles appears in Köhler theory for cloud condensation nuclei (CCN) activation (Köhler 1936). Surface-active agents are abundant in the atmosphere and have been found to lower the surface tension of aqueous aerosol droplets from that of pure water (Shulman et al. 1996; Facchini et al. 1999; Gérard et al. 2016; Petters and Petters 2016). However, in many ways, the exact influence of aerosol surface tension on CCN activation remains an open question and is an active area of research (Farmer et al. 2015; Nozière 2016; Ruehl et al. 2016).

In addition, aerosol particles can have multiple liquid phases, and their morphology can be predicted (at equilibrium) from the interfacial tensions between each phase. Interfacial tension, γ, is the more general term describing the tension at any interface between solids, liquids, or gases. In general, for an aerosol particle at equilibrium consisting of two immiscible liquids ($L1$ and $L2$) suspended in air (G), the angles between the three interfaces (one liquid-liquid and two liquid-gas interfaces) satisfy Neumann's equilibrium condition, which is given as

$$S = \gamma_{L1-G} - (\gamma_{L1-L2} + \gamma_{L2-G}) \quad [8]$$

where S is called the spreading coefficient (Torza and Mason 1970; Reid et al. 2011). If S is positive, in this definition, liquid 2 will spread over liquid 1 spontaneously, thereby forming a core-shell morphology (Kwamena et al. 2010). Thus, determination of the interfacial tensions between the liquids and the surface tensions with air of a multiphase liquid aerosol particle allows a thermodynamic prediction of ambient aerosol morphology.

A recent study demonstrated the use of microfluidic interfacial tension measurements on the aerosol chemical mimics (see Figure 4a) (Metcalf et al. 2016; Boyer and Dutcher 2017). Mixtures of methylglyoxal and formaldehyde in aqueous ammonium sulfate were characterized for their interfacial tension with silicone oil, a proxy (in density and surface tension) for an immiscible organic liquid phase. The study revealed that (1) interfacial tension behaves largely as surface tension with air as measured in an independent study (Sareen et al. 2010), meaning that the microfluidic measurements may be used to assess the surface activity of compounds within the aqueous phase (Boyer and Dutcher 2017); and (2) microfluidic interfacial tension measurements in combination with surface tension measurements to calculate the spreading coefficient indicates that a reactive

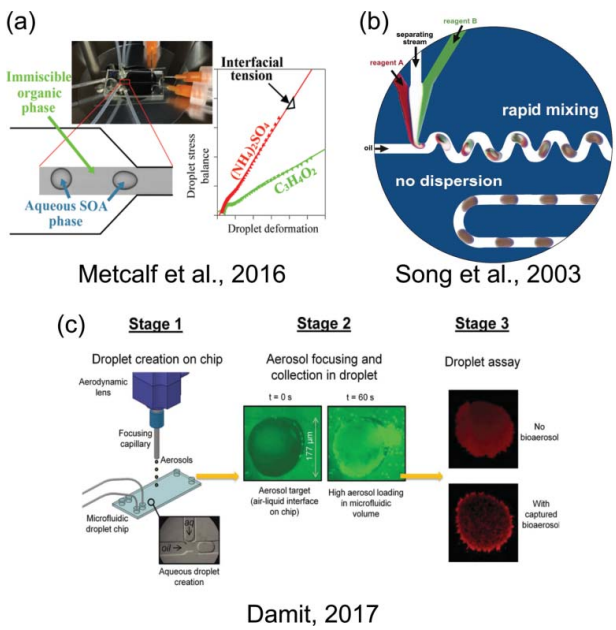

Figure 4. Selected microfluidic chemical and physical measurement techniques. (a) Reprinted with permission from Metcalf, A. R., Boyer, H. C. and Dutcher, C. S. (2016). Interfacial Tensions of Aged Organic Aerosol Particle Mimics Using a Biphasic Microfluidic Platform. Environ. Sci. Technol., 50(3):1251–1259. Copyright 2016 American Chemical Society. (b) Reprinted with permission from Song, H., Tice, J. D. and Ismagilov, R. F. (2003). A Microfluidic System for Controlling Reaction Networks in Time. Angew. Chem., 115(7):792–796. Copyright 2003 WILEY-VCH Verlag GmbH & Co. (c) Reprinted from Damit, B. (2017). Droplet-Based Microfluidics Detector for Bioaerosol Detection. Aerosol Sci. Technol., 51(4):488–500 with permission of the publisher (Taylor & Francis Ltd, http://www.tandfonline.com) and The American Association for Aerosol Research, www.aaar.org.

methylglyoxal-formaldehyde-ammonium sulfate aerosol particle would evolve its morphology if mixed with an immiscible organic liquid (Metcalf et al. 2016).

3.2. Mixing and chemical processing

For experiments requiring little to no mixing or those which seek to examine slower phenomena, residence time in microfluidics devices can be carefully controlled such that the extent of diffusional mixing can be carefully engineered (Brody et al. 1996; Brody and Yager 1997). These are experiments in which the Péclet number is small, allowing diffusional mixing to occur along the length of a flow channel or at the intersection of opposing flows in a cross-slot geometry. Controlled mixing of laminar flows can be used to deliver chemical reactants to, for example, target a single living cell with a reagent at sub-cellular spatial resolution (Takayama et al. 2001) or to control the width of a chemical reaction for the purposes of fabricating a metal wire smaller than 10 μm wide (Kenis et al. 1999). Diffusional mixing can also be exploited to create membrane-less chemical reactors such as fuel cells (Choban et al. 2004). In atmospheric aerosol science, precisely controlled chemical reactions can be exploited to study reaction pathways and mechanisms, especially in aqueous-phase chemistry.

Droplets or slugs of one fluid suspended in another can be used as micro-reactors in which diffusional mixing is aided by internal circulation while a droplet or slug travels along a straight channel (Tice et al. 2003). To hasten mixing within laminar flows, for situations when diffusion alone is too slow, the flow channel geometry is often designed to mimic a "twisted-pipe" configuration, which enables chaotic advection to enhance the mixing process (Aref 1990; Jones et al. 2006). The mixing within droplets or slugs that are used as tiny chemical reactors is greatly enhanced by the mechanical mixing in these channel geometries (see Figure 4b) (Song et al. 2003, 2006). At the microscale, diffusion is enhanced by folding the immiscible fluids onto each other to increase the interfacial area between them over which diffusion can occur (Liu et al. 2000). Mechanical mixing in a twisted pipe or serpentine flow pattern is also known to aerosol scientists; however, this configuration is avoided when possible. In aerosol sampling lines, bends cause secondary flows which mix the carrier gas but also cause increased particle losses to the tubing walls due to an increase in inertial forces acting on the aerosol particles in flow (Tsai and Pui 1990). In contrast, inertia typically does not play a role in microfluidics (Figure 2), meaning that mechanical mixing may be employed in studies to simulate aerosol phase chemistry without wall losses.

Many advanced processing techniques have already been developed for droplet microfluidics. Synthesis of polymeric particles is achieved by forming a droplet of desired shape and size of a precursor liquid followed by curing with various methods (Steinbacher and McQuade 2006). Polymerization can be done by heating (Sugiura et al. 2001a, 2002), UV exposure (Dendukuri et al. 2005; Xu et al. 2005), or interfacial polymerization reactions (Quevedo et al. 2005; Takeuchi et al. 2005). Batch curing can take place while constantly flowing fluid through a microfluidic device and curing with patterned UV exposure, and recent advances have used air-pressure-driven flow to rapidly, temporarily stop the flow to achieve more precise UV exposure (better curing) while maintaining high throughput of the overall particle generation (Dendukuri et al. 2007). Many of these processing techniques may be employed to initiate chemical reactions or other physical phenomena relevant to aerosol science. Because of the small-scale, focused and repeated laser pulses may initiate photochemical reactions in the same way that environmental chambers use UV lights.

3.3. Optical measurements

By far, the majority of microfluidic experiments are performed on a microscope where the most basic on-chip measurement available is visual microscopy; that is, taking an image of the device and fluid flow with an attached camera. Brightfield and darkfield microscopy images rely on a refractive index contrast between immiscible liquid phases or between suspended particles and the surrounding liquid. Brightfield imaging is used to determine interfacial boundaries for physical property measurements. Fluorescence microscopy, on the other hand, typically excites the sample with a pulse of light at one (range of) wavelength(s) and then images at a shorter (range of) wavelength(s) to measure the excitation from the sample. Fluorescence is typically used in biological agent detection; however, a recent study used fluorescence microscopy to image phase-separated atmospheric aerosol (You et al. 2012). In either imaging scenario, high-speed cameras, with frame rates in excess of 10,000 images per second, allow capture of fast, dynamic phenomena, such as interfacial deformation and relaxation.

Microfluidic technology for biological agent detection is gaining popularity due to portability, low fabrication costs, and low reagent consumption. Moreover, microfluidic platforms can integrate analysis with sampling and enrichment into a single lab-on-a-chip device. While this platform has been used extensively for pathogen sensing in a liquid medium for assays, the main challenge in airborne pathogen detection using microfluidics is the introduction of samples into the device (Sackmann

et al. 2014). Several different methods for sampling have been devised, the simplest being direct introduction of the sample into the device using a vacuum pump (Bian et al. 2016). This air sampler, which consists of a double spiral microfluidic channel with a micro-pump at the inlet, is designed to be portable and, hence, convenient for on-site detection of airborne pathogens. The pump aspirates the airflow containing pathogens into the device, and the spiral channel with wave-like and herringbone structures causes them to be trapped in the device. The microfluidic sampler collects and enriches samples much more efficiently than conventional methods, including plate sedimentation of pathogens in a culture medium. A similar design uses a multi-layer PDMS device with S-shaped micro-channels for specific sampling of airborne *mycobacterium tuberculosis* (Jing et al. 2013, 2014). Further, the bacteria collected in the 'enrichment' chip is treated with a buffer solution, which is introduced into a separate 'immunoassay' chip for analysis. In this particular setup, both enrichment of the sample as well as analysis are performed using microfluidics, albeit on two separate chips.

Alternatively, aerodynamic lenses can be used to collect and focus airborne particulate matter onto a microfluidic device (see Figure 4c) (Damit 2017). The aerodynamic lens in this setup serves the function of enriching the air stream with aerosol particles (Novosselov et al. 2014). The aerodynamic lens is followed by a capillary tube, which, in addition to transporting the particles onto the microfluidic device, also exerts air pressure on the open, detection section of the microchannel. This detection port interfaces the droplets inside the microchannel with the air stream from the capillary for collection of aerosol particles into a pinched droplet, similar to an impactor. Droplets formed in the microfluidic device encapsulate particles from the air stream to allow mixing and reaction with known reagents in the droplet followed by fluorescence detection to determine bioaerosol loading.

A third technique for aerosol particle collection and introduction into a microfluidic device is a condensing module, which cools hydrosolized aerosol containing pathogens onto a plate before it is transported to a microfluidic chip for detection of bioluminescence (Lee et al. 2008). Separation of dust particles from airborne pathogens is necessary in order to isolate the pathogens for analysis. Separation has been achieved either by dielectrophoresis (Moon et al. 2009) or by harnessing effects of Dean flow in curved microchannels for inertial separation (Bian et al. 2016).

4. Single particle manipulation

In addition to using microfluidics to characterize fluids and their reaction products, droplet microfluidics may be used to manipulate individual objects through sorting and trapping methods. Highly monodisperse droplets can be rapidly generated and used in experiments which complement existing single-particle experiments employed by aerosol scientists. In this section, on-chip sorting of droplets and particles will be discussed, followed by methods for single particle confinement and manipulation using hydrodynamic and other fields.

4.1. Droplet and particle sorting

Sorting techniques with microfluidic platforms may find applications in screening of aerosol particles by size or chemical composition, with high throughput and significantly reduced residence times. One simple and cost-effective technique, called 'pinched flow fractionation' (PFF) uses a microfluidic device with multiple outlets for sorting droplets based on their size (Maenaka et al. 2008). The incoming sample flow, consisting of a polydisperse emulsion, is pinched by a second flow of pure carrier fluid before entering a wider flow channel (see Figure 5a). The pinching of the flow pushes smaller particles or droplets closer to the wall than larger ones due to particle inertia and drag forces. As the flow profile spreads out in the wider flow channel, the small differences in the positions of these particles become exaggerated, thus facilitating easy separation of droplets by size into multiple outlet channels.

Several techniques similar to pinched-flow fractionation employ hydrodynamic forces alone to achieve size-based separation of deformable droplets and particles (e.g., blood cells) as well as nondeformable particles (e.g., polystyrene beads). For example, a device consisting of curved and cascaded microchannels separates particles based on the principle of inertial focusing; that is, an interaction between Dean drag forces (arising from secondary flow caused by the curvature of the microchannels) and inertial lift forces (responsible for steering particles away from the sides and center of the microchannels) (Di Carlo et al. 2008). A membraneless 'H-filter' is capable of performing size-based separation of particles in parallel laminar flow streams based solely on size-dependent variations in the diffusion coefficient of particles (see Figure 5b) (Brody and Yager 1997; Squires and Quake 2005). For larger particles, the hydrodynamic resistance in a microfluidic channel is greater, leading to so-called 'passive microfluidic circuits' in which variations in hydrodynamic resistance due to particle size induce modulations in flow patterns to achieve size-based separation of particles (Cartas-Ayala et al. 2012).

Apart from size-based sorting, complex techniques for reaction-based sorting are also used by employing external fields. Dielectrophoresis is used to separate mutant

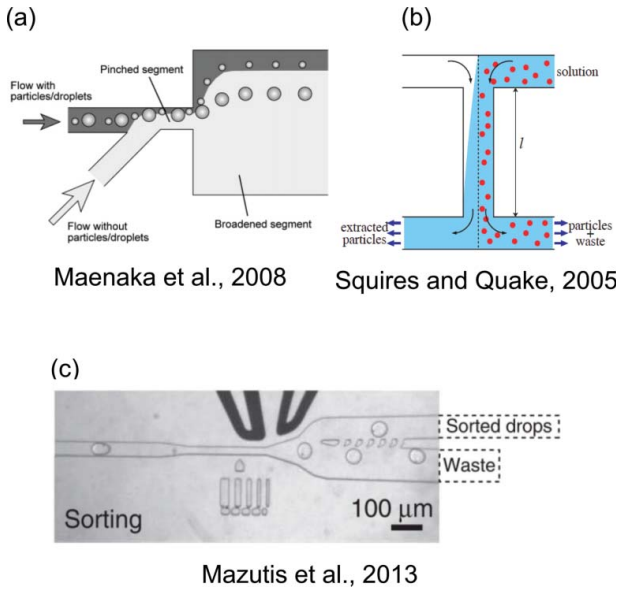

Figure 5. Selected microfluidic droplet and particle sorting techniques. (a) Reprinted with permission from Maenaka, H., Yamada, M., Yasuda, M. and Seki, M. (2008). Continuous and Size-Dependent Sorting of Emulsion Droplets Using Hydrodynamics in Pinched Microchannels. *Langmuir*, 24(8):4405–4410. Copyright 2008 American Chemical Society. (b) Reprinted with permission from Squires, T. M. and Quake, S. R. (2005). Microfluidics: Fluid Physics at the Nanoliter Scale. *Rev. Mod. Phys.*, 77(3):977–1026. Copyright 2005 by the American Physical Society. (c) Adapted by permission from Macmillan Publishers Ltd: Nature Protocols, Mazutis, L., Gilbert, J., Ung, W. L., Weitz, D. A., Griffiths, A. D., and Heyman, J. A. (2013). Single-Cell Analysis and Sorting Using Droplet-Based Microfluidics. Nat. Protoc., 8 (5):870 -891, copyright 2013.

enzymes from cells after activation by a fluorescence intensity-based signal (see Figure 5c) (Agresti et al. 2010; Mazutis et al. 2013). Cells containing the enzymes are encapsulated in aqueous droplets which carry substrates that fluoresce when the reaction commences. If the fluorescence signal from a drop is above a certain threshold value, the sorting electrodes are activated, thereby enabling separation of the mutant enzymes. Several optical techniques employing lasers, including Raman tweezers (Pilát et al. 2014), scanning laser optical trapping (SLOT) (Mio et al. 2000), and diode laser bars (Applegate et al. 2004) can be implemented for efficient and precise sorting of particles.

4.2. Trapping and manipulation

The study and mechanical manipulation of trapped material using flow in hydrodynamic stagnation points goes back at least to 1934 when G. I. Taylor constructed a device called a 'four-roll mill' (Taylor 1934). The four-roll mill was used to study the breakup of macroscopic spherical droplets when subjected to shear and extensional forces. More recently, a microfluidic version of Taylor's four-roll mill was designed to provide superior control over the flow field conditions and to trap microscopic particles at a stagnation point (Hudson et al. 2004). The device consists of six crossing channels arranged in a chiral pattern. However, while extensional flow is readily obtained, shear and rotational flows at the stagnation point are more difficult in small aspect ratio devices (<~2) (Phelan et al. 2005). Improvements to the microfluidic four-roll mill design were achieved with additional geometry creating four in-flow and four out-flow channels which allow all flow types from pure rotation to pure extension to examine microdrop deformation and single molecule dynamics (Lee et al. 2007). Extensional flows are also possible in a much simpler cross-slot geometry (see Figure 6a), a design in which opposing fluid streams create a stagnation point at the center of a four-channel cross (Islam et al. 2004; Pathak and Hudson 2006; Dylla-Spears et al. 2010). A planar extensional flow field at a stagnation point was utilized to trap and extend single molecules of DNA to detect specific sequences in the structure (Dylla-Spears et al. 2010). Microfluidic cross-slot designs have been further optimized to extend

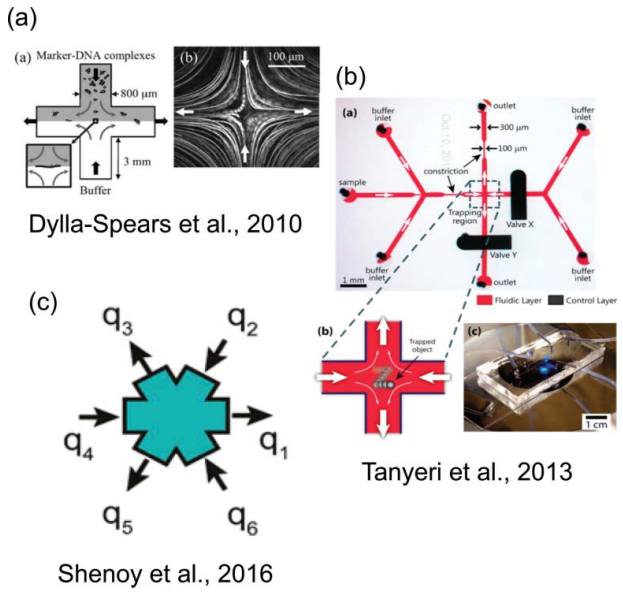

Figure 6. Selected microfluidic trapping and manipulation techniques. (a) Reproduced from Dylla-Spears, R., Townsend, J. E., Jen-Jacobson, L., Sohn, L. L. and Muller, S. J. (2010). Single-Molecule Sequence Detection via Microfluidic Planar Extensional Flow at a Stagnation Point. *Lab Chip*, 10(12):1543–1549 with permission of The Royal Society of Chemistry. (b) Reprinted with permission from Tanyeri, M. and Schroeder, C. M. (2013). Manipulation and Confinement of Single Particles Using Fluid Flow. *Nano Lett.*, 13(6):2357–2364. Copyright 2013 American Chemical Society. (c) Reprinted with permission from Shenoy, A., Rao, C. V. and Schroeder, C. M. (2016). Stokes Trap for Multiplexed Particle Manipulation and Assembly Using Fluidics. *Proc. Natl. Acad. Sci. U. S. A.*, 113(15):3976–3981.

the region of homogeneous extensional strain over a larger area (Haward et al. 2012; Galindo-Rosales et al. 2014). Fine control of the stagnation point is facilitated by fabricating a two-layer PDMS device (see Figure 6b) (Tanyeri and Schroeder 2013).

Growing interest in stagnation point flows in microfluidic devices was driven by the ability of such devices to effectively trap single cells, molecules, droplets, bubbles, and vesicles for study of their properties. Hydrodynamic traps allow nonperturbative, noncontact, fine-scale confinement and manipulation of single droplets or particles for long periods of time (Tanyeri et al. 2011; Tanyeri and Schroeder 2013). Particles are trapped in continuously flowing solution, allowing for rapid changes of the surrounding medium to be made during experiments. "Hydrodynamic tweezers" employing microeddies have also been used to gently trap and position single cells for analysis in a microfluidic device without artificially affecting their behavior (Lutz et al. 2006). A recently developed microfluidic "Stokes Trap" (see Figure 6c) is capable of trapping one or more colloidal particles in a four or six-channel trap design with multiple stagnation points (Shenoy et al. 2016). Trapping is achieved by implementing an optimization algorithm to exert fine-scale control over the pressures in fluidic reservoirs in a pressure-driven flow system, without the need for a separate control layer on the microfluidic chip. The flexibility afforded by the Stokes trap design has tremendous potential, not just for confining multiple particles, but also for studying the dynamics of droplet coalescence. A hydrodynamic trap can trap particles of an arbitrary physicochemical complexity and serves as a complementary technique to alternative single-particle methods using optical, electric, magnetic, or acoustic fields for confinement (see Table 2).

5. Outlook

In the field of aerosol science, microfluidic flows and devices are largely underused, yet potentially transformative to the field (see Table 3 for potential applications). Biphasic microfluidics can be used to sort, process, trap, and manipulate droplets and particles for chemical and physical measurements. Because microfluidic devices most often use liquid phases, a Particle-into-Liquid Sampler (PILS) (Weber et al. 2001; Sorooshian et al. 2006) could be used for collection of ambient water-soluble aerosol species for microfluidic measurements. PILS instruments have been used for vial collection for offline analyses (Bateman et al. 2010) and for online measurements by coupling to a Total Organic Carbon analyzer (Sullivan et al. 2004) or in conjunction with mass spectrometry to detect tracers from biomass burning in ambient aerosols (Saarnio et al. 2013). Both offline and online modes of the PILS could be adapted for microfluidic measurements to take advantage of the small sample volumes required for typical microfluidic experiments.

Table 3. Selected microfluidic techniques and potential aerosol science applications.

Microfluidic Technique	Potential Application to Aerosol Science
Temperature control/gradients	Ice nucleation studies
Chemical gradients	Bioaerosol studies; heterogeneous chemistry
Electric fields	Electrophoretic mobility
Droplet/particle sorting	Particle size separation
Trapping and manipulation	Single-particle studies; thermodynamic and physical characterization
Diffusional mixing	Heterogeneous chemistry
Designer emulsions	Generate aerosol standards

Another future direction of these fields might be to further integrate microfluidic techniques with ambient aerosol sampling. While particle impaction onto a digital microfluidic device is already in use, as discussed above, more work can be done to refine these techniques with an aerodynamic lens for concentrating the aerosol. Integration with a spot sampler to grow smaller particles for a wider size range of impaction onto microfluidic devices may greatly enhance the sampling capabilities of these devices (Eiguren-Fernandez et al. 2014).

When using either collected samples or chemical mimics of atmospheric aerosols, a number of new avenues of study will be available, offering advantages over traditional aerosol techniques. These advantages include low fabrication costs, rapid repeatability of experiments, fast equilibration times, and single-droplet, noncontact methods for experimentation.

Acknowledgments

We gratefully acknowledge Prof. Gordon Christopher for sharing device design files to aid in the startup of this project, and Prof. Kevin Dorfman for allowing use of his laboratory and equipment for fabrication of PDMS microfluidic devices. We also thank Drs. Zhicheng Long, Christopher Nelson, and Rebecca Dylla-Spears, and Profs. Shelley Anna, Lynn Walker, and Charles Schroeder for useful discussions. We acknowledge Harry Barrett for collection of most of the data in Figure S2 and Donaldson Company, Inc. for use of their SEM for the images in Figure 1. We thank Peter McMurry for useful comments on the manuscript.

Funding

Part of this work was carried out in the College of Science and Engineering Minnesota Nano Center, University of Minnesota, which receives partial support from NSF through the NNIN

program. C.S.D. was partially supported by a 3M Nontenure Faculty Award. This material is based upon work supported by the National Science Foundation under Grant Number AGS-1433514 and CAREER Grant Number 1554936.

ORCID

Andrew R. Metcalf http://orcid.org/0000-0003-0385-1356
Shweta Narayan http://orcid.org/0000-0003-1829-365X
Cari S. Dutcher http://orcid.org/0000-0003-4325-9197

References

Abate, A. R., and Weitz, D. A. (2009). High-Order Multiple Emulsions Formed in Poly(Dimethylsiloxane) Microfluidics. *Small*, 5(18):2030–2032. doi:10.1002/smll.200900569.

Abdelgawad, M., and Wheeler, A. R. (2009). The Digital Revolution: A New Paradigm for Microfluidics. *Adv. Mater.*, 21 (8):920–925. doi:10.1002/adma.200802244.

Agresti, J. J., Antipov, E., Abate, A. R., Ahn, K., Rowat, A. C., Baret, J. C., Márquez, M., Klibanov, A. M., Griffiths, A. D., and Weitz, D. A. (2010). Ultrahigh-Throughput Screening in Drop-Based Microfluidics for Directed Evolution. *Proc. Natl. Acad. Sci. U. S. A.*, 107(9):4004–4009. doi:10.1073/pnas.0910781107.

Ahn, K., Kerbage, C., Hunt, T. P., Westervelt, R. M., Link, D. R., and Weitz, D. A. (2006). Dielectrophoretic Manipulation of Drops for High-Speed Microfluidic Sorting Devices. *Appl. Phys. Lett.*, 88:024104. doi:10.1063/1.2164911.

Alvarez, N. J., Vogus, D. R., Walker, L. M., and Anna, S. L. (2012). Using Bulk Convection in a Microtensiometer to Approach Kinetic-Limited Surfactant Dynamics at Fluid–Fluid Interfaces. *J. Colloid Interface Sci.*, 372(1):183–191. doi:10.1016/j.jcis.2011.12.034.

Amstad, E., Gopinadhan, M., Holtze, C., Osuji, C. O., Brenner, M. P., Spaepen, F., and Weitz, D. A. (2015). Production of Amorphous Nanoparticles by Supersonic Spray-Drying with a Microfluidic Nebulator. *Science*, 349(6251):956–960. doi:10.1126/science.aac9582.

Amstad, E., Spaepen, F., Brenner, M., and Weitz, D. A. (2017). The Microfluidic Nebulator: Production of Sub-Micrometer Sized Airborne Drops. *Lab Chip*, 453(8):253–1480. doi:10.1039/c6lc01455k.

Anna, S. L. (2016). Droplets and Bubbles in Microfluidic Devices. *Annu. Rev. Fluid Mech.*, 48(1):285–309. doi:10.1146/annurev-fluid-122414-034425.

Anna, S. L., Bontoux, N., and Stone, H. A. (2003). Formation of Dispersions Using "Flow Focusing" in Microchannels. *Appl. Phys. Lett.*, 82(3):364. doi:10.1063/1.1537519.

Applegate, R. W., Squier, J., Vestad, T., Oakey, J., and Marr, D. W. M. (2004). Optical Trapping, Manipulation, and Sorting of Cells and Colloids in Microfluidic Systems with Diode Laser Bars. *Opt. Express*, 12(19):4390–4398. doi:10.1364/OPEX.12.004390.

Aref, H. (1990). Chaotic Advection of Fluid Particles. *Philos. Trans. R. Soc., A*, 333(1631):273–288. doi:10.1098/rsta.1990.0161.

Ashkin, A., Dziedzic, J. M., Bjorkholm, J. E., and Chu, S. (1986). Observation of a Single-Beam Gradient Force Optical Trap for Dielectric Particles. *Opt. Lett.*, 11(5):288. doi:10.1364/OL.11.000288.

Baldelli, A., Power, R. M., Miles, R. E. H., Reid, J. P., and Vehring, R. (2016). Effect of Crystallization Kinetics on the Properties of Spray Dried Microparticles. *Aerosol Sci. Technol.*, 50(7):693–704. doi:10.1080/02786826.2016.1177163.

Barca, F., Caporossi, T., and Rizzo, S. (2014). Silicone Oil: Different Physical Proprieties and Clinical Applications. *BioMed Res. Int.*, 2014(5):1–7. doi:10.1155/2014/502143.

Baroud, C. N., Robert de Saint Vincent, M., and Delville, J.-P. (2007). An Optical Toolbox for Total Control of Droplet Microfluidics. *Lab Chip*, 7(8):1029–5. doi:10.1039/b702472j.

Bateman, A. P., Nizkorodov, S. A., Laskin, J., and Laskin, A. (2010). High-Resolution Electrospray Ionization Mass Spectrometry Analysis of Water-Soluble Organic Aerosols Collected with a Particle Into Liquid Sampler. *Anal. Chem.*, 82(19):8010–8016. doi:10.1021/ac1014386.

Baustian, K. J., Cziczo, D. J., Wise, M. E., Pratt, K. A., Kulkarni, G., Hallar, A. G., and Tolbert, M. A. (2012). Importance of Aerosol Composition, Mixing State, and Morphology for Heterogeneous Ice Nucleation: a Combined Field and Laboratory Approach. *J. Geophys. Res.*, 117:D06217. doi:10.1029/2011JD016784.

Berglund, R. N., and Liu, B. Y. H. (1973). Generation of Monodisperse Aerosol Standards. *Environ. Sci. Technol.*, 7 (2):147–153.

Berry, J. D., Neeson, M. J., Dagastine, R. R., Chan, D. Y. C., and Tabor, R. F. (2015). Measurement of Surface and Interfacial Tension Using Pendant Drop Tensiometry. *J. Colloid Interface Sci.*, 454:226–237. doi:10.1016/j.jcis.2015.05.012.

Bertram, A. K., Ivanov, A. V., Hunter, M., Molina, L. T., and Molina, M. J. (2001). The Reaction Probability of OH on Organic Surfaces of Tropospheric Interest. *J. Phys. Chem. A*, 105(41):9415–9421. doi:10.1021/jp0114034.

Bian, X., Lan, Y., Wang, B., Zhang, Y. S., Liu, B., Yang, P., Zhang, W., and Qiao, L. (2016). Microfluidic Air Sampler for Highly Efficient Bacterial Aerosol Collection and Identification. *Anal. Chem.*, 88(23):11504–11512. doi:10.1021/acs.analchem.6b02708.

Bong, K. W., Chapin, S. C., Pregibon, D. C., Baah, D., Floyd-Smith, T. M., and Doyle, P. S. (2011). Compressed-Air Flow Control System. *Lab Chip*, 11(4):743–747. doi:10.1039/c0lc00303d.

Boyer, H. C., and Dutcher, C. S. (2017). Atmospheric Aqueous Aerosol Surface Tensions: Isotherm-Based Modeling and Biphasic Microfluidic Measurements. *J. Phys. Chem. A*, 121 (25):4733–4742. doi:10.1021/acs.jpca.7b03189.

Brody, J. P., and Yager, P. (1997). Diffusion-Based Extraction in a Microfabricated Device. *Sens. Actuators A Phys.*, 58 (1):13–18. doi:10.1016/S0924-4247(97)80219-1.

Brody, J. P., Osborn, T. D., Forster, F. K., and Yager, P. (1996). A Planar Microfabricated Fluid Filter. *Sens. Actuators, A Phys.*, 54(1–3):704–708. doi:10.1016/S0924-4247(97)80042-8.

Bruus, H. (2011). *Theoretical Microfluidics*. Oxford University Press, New York. doi:10.1002/3527601953.ch8/summary.

Bzdek, B. R., Power, R. M., Simpson, S. H., Reid, J. P., and Royall, C. P. (2016). Precise, Contactless Measurements of the Surface Tension of Picolitre Aerosol Droplets. *Chem. Sci.*, 7 (1):274–285. doi:10.1039/C5SC03184B.

Cartas-Ayala, M. A., Raafat, M., and Karnik, R. (2012). Self-Sorting of Deformable Particles in an Asynchronous Logic

Microfluidic Circuit. *Small*, 9(3):375–381. doi:10.1002/smll.201201422.

Chen, B. T., Cheng, Y. S., and Yeh, H. C. (2007). Performance of a TSI Aerodynamic Particle Sizer. *Aerosol Sci. Technol.*, 4 (1):89–97. doi:10.1080/02786828508959041.

Chen, D. R., Pui, D. Y. H., Hummes, D., Fissan, H., Quant, F. R., and Sem, G. J. (1998). Design and Evaluation of a Nanometer Aerosol Differential Mobility Analyzer (Nano-DMA). *J. Aerosol Sci.*, 29(5,6):497–509. doi:10.1016/S0021-8502(97)10018-0.

Choban, E. R., Markoski, L. J., Wieckowski, A., and Kenis, P. J. A. (2004). Microfluidic Fuel Cell Based on Laminar Flow. *J. Power Sources*, 128(1):54–60. doi:10.1016/j.jpowsour.2003.11.052.

Christopher, G. F., and Anna, S. L. (2007). Microfluidic Methods for Generating Continuous Droplet Streams. *J. Phys. D: Appl. Phys.*, 40(19):R319–R336. doi:10.1088/0022-3727/40/19/R01.

Christopher, G. F., Noharuddin, N. N., Taylor, J. A., and Anna, S. L. (2008). Experimental Observations of the Squeezing-to-Dripping Transition in T-Shaped Microfluidic Junctions. *Phys. Rev. E*, 78(3):036317. doi:10.1103/PhysRevE.78.036317.

Chu, L.-Y., Kim, J.-W., Shah, R. K., and Weitz, D. A. (2007a). Monodisperse Thermoresponsive Microgels with Tunable Volume-Phase Transition Kinetics. *Adv. Funct. Mater.*, 17 (17):3499–3504. doi:10.1002/adfm.200700379.

Chu, L.-Y., Utada, A. S., Shah, R. K., Kim, J.-W., and Weitz, D. A. (2007b). Controllable Monodisperse Multiple Emulsions. *Angew. Chem., Int. Ed.*, 46(47):8970–8974. doi:10.1002/anie.200701358.

Cloupeau, M., and Prunet-Foch, B. (1994). Electrohydrodynamic Spraying Functioning Modes: A Critical Review. *J. Aerosol Sci.*, 25(6):1021–1036. doi:10.1016/0021-8502(94)90199-6.

Cocker, D. R., Flagan, R. C., and Seinfeld, J. H. (2001). State-of-the-Art Chamber Facility for Studying Atmospheric Aerosol Chemistry. *Environ. Sci. Technol.*, 35(12):2594–2601. doi:10.1021/es0019169.

Colberg, C. A., Krieger, U. K., and Peter, T. (2004). Morphological Investigations of Single Levitated $H_2SO_4/NH_3/H_2O$ Aerosol Particles During Deliquescence/Efflorescence Experiments. *J. Phys. Chem. A*, 108(14):2700–2709. doi:10.1021/jp037628r.

Cross, E. S., Slowik, J. G., Davidovits, P., Allan, J. D., Worsnop, D. R., Jayne, J. T., Lewis, D. K., Canagaratna, M. R., and Onasch, T. B. (2007). Laboratory and Ambient Particle Density Determinations Using Light Scattering in Conjunction with Aerosol Mass Spectrometry. *Aerosol Sci. Technol.*, 41(4):343–359. doi:10.1080/02786820701199736.

Damit, B. (2017). Droplet-Based Microfluidics Detector for Bioaerosol Detection. *Aerosol Sci. Technol.*, 51(4):488–500. doi:10.1080/02786826.2016.1275515.

Davies, J. F., Haddrell, A. E., and Reid, J. P. (2012). Time-Resolved Measurements of the Evaporation of Volatile Components From Single Aerosol Droplets. *Aerosol Sci. Technol.*, 46(6):666–677. doi:10.1080/02786826.2011.652750.

Davies, J. F., Miles, R. E. H., Haddrell, A. E., and Reid, J. P. (2013). Influence of Organic Films on the Evaporation and Condensation of Water in Aerosol. *Proc. Natl. Acad. Sci. U. S. A.*, 110(22):8807–8812. doi:10.1073/pnas.1305277110.

Davies, J. T., and Rideal, E. K. (1963). *Interfacial Phenomena*. Second Edition. Academic Press, New York.

Davis, E. J. (1997). A History of Single Aerosol Particle Levitation. *Aerosol Sci. Technol.*, 26(3):212–254. doi:10.1080/02786829708965426.

Davis, E. J., Buehler, M. F., and Ward, T. L. (1990). The Double-Ring Electrodynamic Balance for Microparticle Characterization. *Rev. Sci. Instrum.*, 61(4):1281–1288. doi:10.1063/1.1141227.

Dendukuri, D., Gu, S. S., Pregibon, D. C., Hatton, T. A., and Doyle, P. S. (2007). Stop-Flow Lithography in a Microfluidic Device. *Lab Chip*, 7(7):818. doi:10.1039/b703457a.

Dendukuri, D., Tsoi, K., Hatton, T. A., and Doyle, P. S. (2005). Controlled Synthesis of Nonspherical Microparticles Using Microfluidics. *Langmuir*, 21(6):2113–2116. doi:10.1021/la047368k.

Di Carlo, D., Edd, J. F., Irimia, D., Tompkins, R. G., and Toner, M. (2008). Equilibrium Separation and Filtration of Particles Using Differential Inertial Focusing. *Anal. Chem.*, 80 (6):2204–2211. doi:10.1021/ac702283m.

Dubinsky, S., Zhang, H., Nie, Z., Gourevich, I., Voicu, D., Deetz, M., and Kumacheva, E. (2008). Microfluidic Synthesis of Macroporous Copolymer Particles. *Macromolecules*, 41(10):3555–3561. doi:10.1021/ma800300d.

Duncanson, W. J., Zieringer, M., Wagner, O., Wilking, J. N., Abbaspourrad, A., Haag, R., and Weitz, D. A. (2012). Microfluidic Synthesis of Monodisperse Porous Microspheres with Size-Tunable Pores. *Soft Matter*, 8(41):10636–10640. doi:10.1039/C2SM25694K.

Dylla-Spears, R., Townsend, J. E., Jen-Jacobson, L., Sohn, L. L., and Muller, S. J. (2010). Single-Molecule Sequence Detection via Microfluidic Planar Extensional Flow at a Stagnation Point. *Lab Chip*, 10(12):1543–1549. doi:10.1039/B926847B.

Ehara, K., Hagwood, C., and Coakley, K. J. (1996). Novel Method to Classify Aerosol Particles According to Their Mass-to-Charge Ratio—Aerosol Particle Mass Analyser. *J. Aerosol Sci.*, 27(2):217–234. doi:10.1016/0021-8502(95)00562-5.

Eiguren-Fernandez, A., Lewis, G. S., and Hering, S. V. (2014). Design and Laboratory Evaluation of a Sequential Spot Sampler for Time-Resolved Measurement of Airborne Particle Composition. *Aerosol Sci. Technol.*, 48(6):655–663. doi:10.1080/02786826.2014.911409.

Erickson, D., and Li, D. (2004). Integrated Microfluidic Devices. *Anal. Chim. Acta*, 507(1):11–26. doi:10.1016/j.aca.2003.09.019.

Facchini, M. C., Mircea, M., Fuzzi, S., and Charlson, R. J. (1999). Cloud Albedo Enhancement by Surface-Active Organic Solutes in Growing Droplets. *Nature*, 401 (6750):257–259. doi:10.1038/45758.

Fair, R. B., Khlystov, A., Srinivasan, V., Pamula, V. K., and Weaver, K. N. (2004). Integrated Chemical/Biochemical Sample Collection, Pre-Concentration, and Analysis on a Digital Microfluidic Lab-on-a-Chip Platform. Edited by Linda A Smith and Daniel Sobek. *Proc. SPIE*, 5591:113–124. doi:10.1117/12.581955.

Fair, R. B., Khlystov, A., Tailor, T. D., Ivanov, V., Evans, R. D., Srinivasan, V., Pamula, V. K., Pollack, M. G., Griffin, P. B., and Zhou, J. (2007). Chemical and Biological Applications of Digital-Microfluidic Devices. *IEEE Des. Test Comput.*, 24 (1):10–24. doi:10.1109/MDT.2007.8.

Farmer, D. K., Cappa, C. D., and Kreidenweis, S. M. (2015). Atmospheric Processes and Their Controlling Influence on Cloud Condensation Nuclei Activity. *Chem. Rev.*, 115 (10):4199–4217. doi:10.1021/cr5006292.

Fernández-Nieves, A., Vitelli, V., Utada, A. S., Link, D. R., Márquez, M., Nelson, D. R., and Weitz, D. A. (2007). Novel Defect Structures in Nematic Liquid Crystal Shells. *Phys. Rev. Lett.*, 99(15):157801. doi:10.1103/PhysRevLett.99.157801.

Folkers, M., Mentel, T. F., and Wahner, A. (2003). Influence of an Organic Coating on the Reactivity of Aqueous Aerosols Probed by the Heterogeneous Hydrolysis of N_2O_5. *Geophys. Res. Lett.*, 30(12):1644. doi:10.1029/2003GL017168.

Freedman, M. A., Baustian, K. J., Wise, M. E., and Tolbert, M. A. (2010). Characterizing the Morphology of Organic Aerosols at Ambient Temperature and Pressure. *Anal. Chem.*, 82 (19):7965–7972. doi:10.1021/ac101437w.

Freney, E. J., Adachi, K., and Buseck, P. R. (2010). Internally Mixed Atmospheric Aerosol Particles: Hygroscopic Growth and Light Scattering. *J. Geophys. Res.*, 115(D19):D19210. doi:10.1029/2009JD013558.

Gad-el-Hak, M. (1999). The Fluid Mechanics of Microdevices—the Freeman Scholar Lecture. *J. Fluids Eng.*, 121(1):5–33. doi:10.1115/1.2822013.

Galindo-Rosales, F. J., Oliveira, M. S. N., and Alves, M. A. (2014). Optimized Cross-Slot Microdevices for Homogeneous Extension. *RSC Adv.*, 4(15):7799–7804. doi:10.1039/C3RA47230B.

Garstecki, P., Fuerstman, M. J., Stone, H. A., and Whitesides, G. M. (2006). Formation of Droplets and Bubbles in a Microfluidic T-Junction—Scaling and Mechanism of Break-Up. *Lab Chip*, 6(3):437–446. doi:10.1039/B510841A.

Garstecki, P., Stone, H. A., and Whitesides, G. (2005). Mechanism for Flow-Rate Controlled Breakup in Confined Geometries: a Route to Monodisperse Emulsions. *Phys. Rev. Lett.*, 94(16):164501. doi:10.1103/PhysRevLett.94.164501.

George, I. J., and Abbatt, J. P. D. (2010). Heterogeneous Oxidation of Atmospheric Aerosol Particles by Gas-Phase Radicals. *Nat. Chem.*, 2(9):713–722. doi:10.1038/nchem.806.

Gérard, V., Nozière, B., Baduel, C., Fine, L., Frossard, A. A., and Cohen, R. C. (2016). Anionic, Cationic, and Nonionic Surfactants in Atmospheric Aerosols From the Baltic Coast at Askö, Sweden: Implications for Cloud Droplet Activation. *Environ. Sci. Technol.*, 50(6):2974–2982. doi:10.1021/acs.est.5b05809.

Grace, J. M., and Marijnissen, J. C. M. (1994). A Review of Liquid Atomization by Electrical Means. *J. Aerosol Sci.*, 25 (6):1005–1019. doi:10.1016/0021-8502(94)90198-8.

Gravesen, P., Branebjerg, J., and Jensen, O. S. (1993). Microfluidics-a Review. *J. Micromech. Microeng.*, 3(4):168–182. doi:10.1088/0960-1317/3/4/002.

Gupta, R., Hindle, M., Byron, P. R., Cox, K. A., and McRae, D. D. (2003). Investigation of a Novel Condensation Aerosol Generator: Solute and Solvent Effects. *Aerosol Sci. Technol.*, 37(8):672–681. doi:10.1080/02786820300910.

Haward, S. J., Oliveira, M. S. N., Alves, M. A., and McKinley, G. H. (2012). Optimized Cross-Slot Flow Geometry for Microfluidic Extensional Rheometry. *Phys. Rev. Lett.*, 109(12):128301. doi:10.1103/PhysRevLett.109.128301.

Hayward, R. C., Utada, A. S., Dan, N., and Weitz, D. A. (2006). Dewetting Instability During the Formation of Polymersomes From Block-Copolymer-Stabilized Double Emulsions. *Langmuir*, 22(10):4457–4461. doi:10.1021/la060094b.

Hinds, W. C. (1999). *Aerosol Technology*. Second Edition. John Wiley & Sons, Inc, New York.

Hudson, S. D., Phelan, F. R., Jr., Handler, M. D., Cabral, J. T., Migler, K. B., and Amis, E. J. (2004). Microfluidic Analog of the Four-Roll Mill. *Appl. Phys. Lett.*, 85(2):335–337. doi:10.1063/1.1767594.

Islam, M. T., Vanapalli, S. A., and Solomon, M. J. (2004). Inertial Effects on Polymer Chain Scission in Planar Elongational Cross-Slot Flow. *Macromolecules*, 37(3):1023–1030. doi:10.1021/ma035254u.

Jebrail, M. J., Bartsch, M. S., and Patel, K. D. (2012). Digital Microfluidics: a Versatile Tool for Applications in Chemistry, Biology and Medicine. *Lab Chip*, 12(14):2452–13. doi:10.1039/c2lc40318h.

Jebrail, M. J., Yang, H., Mudrik, J. M., Lafreni re, N. M., McRoberts, C., Al-Dirbashi, O. Y., Fisher, L., Chakraborty, P., and Wheeler, A. R. (2011). A Digital Microfluidic Method for Dried Blood Spot Analysis. *Lab Chip*, 11(19):3218. doi:10.1039/c1lc20524b.

Jeon, N., Baskaran, H., Dertinger, S. K. W., Whitesides, G. M., Van De Water, L., and Toner, M. (2002). Neutrophil Chemotaxis in Linear and Complex Gradients of Interleukin-8 Formed in a Microfabricated Device. *Nat. Biotechnol.*, 20 (8):826–830. doi:10.1038/nbt712.

Jing, W., Jiang, X., Zhao, W., Liu, S., Cheng, X., and Sui, G. (2014). Microfluidic Platform for Direct Capture and Analysis of Airborne Mycobacterium Tuberculosis. *Anal. Chem.*, 86(12):5815–5821. doi:10.1021/ac500578h.

Jing, W., Zhao, W., Liu, S., Li, L., Tsai, C.-T., Fan, X., Wu, W., Li, J., Yang, X., and Sui, G. (2013). Microfluidic Device for Efficient Airborne Bacteria Capture and Enrichment. *Anal. Chem.*, 85(10):5255–5262. doi:10.1021/ac400590c.

Jones, S. W., Thomas, O. M., and Aref, H. (2006). Chaotic Advection by Laminar Flow in a Twisted Pipe. *J. Fluid Mech.*, 209:335–357. doi:10.1017/S0022112089003137.

Karam, P., Dukhin, A., and Pennathur, S. (2017). Optimal MEMS Device for Mobility and Zeta Potential Measurements Using DC Electrophoresis. *Electrophoresis.*, 38:1245–1250. doi:10.1002/elps.201700029.

Kawakatsu, T., Trägårdh, G., Trägårdh, C., Nakajima, M., Oda, N., and Yonemoto, T. (2001). The Effect of the Hydrophobicity of Microchannels and Components in Water and Oil Phases on Droplet Formation in Microchannel Water-in-Oil Emulsification. *Colloid Surface A*, 179(1):29–37. doi:10.1016/S0927-7757(00)00498-2.

Kenis, P. J. A., Ismagilov, R. F., and Whitesides, G. M. (1999). Microfabrication Inside Capillaries Using Multiphase Laminar Flow Patterning. *Science*, 285(5424):83–85. doi:10.1126/science.285.5424.83.

Kim, J.-W., Utada, A. S., Fernández-Nieves, A., Hu, Z., and Weitz, D. A. (2007). Fabrication of Monodisperse Gel Shells and Functional Microgels in Microfluidic Devices. *Angew. Chem.*, 119(11):1851–1854. doi:10.1002/ange.200604206.

Kirby, A. E., and Wheeler, A. R. (2013). Digital Microfluidics: an Emerging Sample Preparation Platform for Mass Spectrometry. *Anal. Chem.*, 85(13):6178–6184. doi:10.1021/ac401150q.

Knutson, E. O., and Whitby, K. T. (1975). Aerosol Classification by Electric Mobility: Apparatus, Theory, and Applications. *J. Aerosol Sci.*, 6(6):443–451. doi:10.1016/0021-8502(75)90060-9.

Kobayashi, I., Nakajima, M., Tong, J., Kawakatsu, T., Nabetani, H., Kikuchi, Y., Shohno, A., and Satho, K. (1999).

Production and Characterization of Monodispersed Oil-in-Water Microspheres Using Microchannels. *Food Sci. Technol. Res.*, 5(4):350–355. doi:10.3136/fstr.5.350.

Köhler, H. (1936). The Nucleus in and the Growth of Hygroscopic Droplets. *Trans. Faraday Soc.*, 32(0):1152–1161. doi:10.1039/TF9363201152.

Kramer, A. J., Rattanavaraha, W., Zhang, Z., Gold, A., Surratt, J. D., and Lin, Y.-H. (2016). Assessing the Oxidative Potential of Isoprene-Derived Epoxides and Secondary Organic Aerosol. *Atmos. Environ.*, 130:211–218. doi:10.1016/j.atmosenv.2015.10.018.

Kulkarni, P., Baron, P. A., and Willeke, K., eds. (2011). *Aerosol Measurement*. Third Edition. John Wiley & Sons, Inc.

Kwamena, N. O. A., Buajarern, J., and Reid, J. P. (2010). Equilibrium Morphology of Mixed Organic/Inorganic/Aqueous Aerosol Droplets: Investigating the Effect of Relative Humidity and Surfactants. *J. Phys. Chem. A*, 114(18):5787–5795. doi:10.1021/jp1003648.

Lee, D., Fang, C., Ravan, A. S., Fuller, G. G., and Shen, A. Q. (2017). Temperature Controlled Tensiometry Using Droplet Microfluidics. *Lab Chip*, 17(4):717–726. doi:10.1039/C6LC01384H.

Lee, J. S., Dylla-Spears, R., Teclemariam, N. P., and Muller, S. J. (2007). Microfluidic Four-Roll Mill for All Flow Types. *Appl. Phys. Lett.*, 90(7):074103. doi:10.1063/1.2472528.

Lee, S., Park, J., Im, H., and Jung, H.-I. (2008). A Microfluidic ATP-Bioluminescence Sensor for the Detection of Airborne Microbes. *Sens. Actuat. B-Chem.*, 132(2):443–448. doi:10.1016/j.snb.2007.10.035.

Li, C.-W., Chen, R., and Yang, M. (2007). Generation of Linear and Non-Linear Concentration Gradients Along Microfluidic Channel by Microtunnel Controlled Stepwise Addition of Sample Solution. *Lab Chip*, 7(10):1371–1373. doi:10.1039/b705525k.

Li, Z., Schwier, A. N., Sareen, N., and McNeill, V. F. (2011). Reactive Processing of Formaldehyde and Acetaldehyde in Aqueous Aerosol Mimics: Surface Tension Depression and Secondary Organic Products. *Atmos. Chem. Phys.*, 11(22):11617–11629. doi:10.5194/acp-11-11617-2011.

Lin, Y.-H., Zhang, Z., Docherty, K. S., Zhang, H., Budisulistiorini, S. H., Rubitschun, C. L., Shaw, S. L., Knipping, E. M., Edgerton, E. S., Kleindienst, T. E., Gold, A., and Surratt, J. D. (2012). Isoprene Epoxydiols as Precursors to Secondary Organic Aerosol Formation: Acid-Catalyzed Reactive Uptake Studies with Authentic Compounds. *Environ. Sci. Technol.*, 46(1):250–258. doi:10.1021/es202554c.

Liu, B. Y. H., and Lee, K. W. (1975). An Aerosol Generator of High Stability. *Am. Ind. Hyg. Assoc. J.*, 36(12):861–865. doi:10.1080/0002889758507357.

Liu, B. Y. H., and Pui, D. Y. H. (1975). On the Performance of the Electrical Aerosol Analyzer. *J. Aerosol Sci.*, 6(3–4):249–254. doi:10.1016/0021-8502(75)90093-2.

Liu, B. Y. H., Romay, F. J., Dick, W. D., Woo, K.-S., and Chiruta, M. (2010). A Wide-Range Particle Spectrometer for Aerosol Measurement From 0.010 Mm to 10 Mm. *Aerosol Air Qual. Res.*, 10(2):125–139. doi:10.4209/aaqr.2009.10.0062.

Liu, P., Ziemann, P. J., Kittelson, D. B., and McMurry, P. H. (1995). Generating Particle Beams of Controlled Dimensions and Divergence: II. Experimental Evaluation of Particle Motion in Aerodynamic Lenses and Nozzle Expansions. *Aerosol Sci. Technol.*, 22(3):314–324. doi:10.1080/02786829408959749.

Liu, R. H., Stremler, M. A., Sharp, K. V., Olsen, M. G., Santiago, J. G., Adrian, R. J., Aref, H., and Beebe, D. J. (2000). Passive Mixing in a Three-Dimensional Serpentine Microchannel. *J. Microelectromech. Syst.*, 9(2):190–197. doi:10.1109/84.846699.

Lutz, B. R., Chen, J., and Schwartz, D. T. (2006). Hydrodynamic Tweezers: 1. Noncontact Trapping of Single Cells Using Steady Streaming Microeddies. *Anal. Chem.*, 78(15):5429–5435. doi:10.1021/ac060555y.

Maenaka, H., Yamada, M., Yasuda, M., and Seki, M. (2008). Continuous and Size-Dependent Sorting of Emulsion Droplets Using Hydrodynamics in Pinched Microchannels. *Langmuir*, 24(8):4405–4410. doi:10.1021/la703581j.

Mazutis, L., Gilbert, J., Ung, W. L., Weitz, D. A., Griffiths, A. D., and Heyman, J. A. (2013). Single-Cell Analysis and Sorting Using Droplet-Based Microfluidics. *Nat Protoc*, 8(5):870–891. doi:10.1038/nprot.2013.046.

McNeill, V. F., Patterson, J., Wolfe, G. M., and Thornton, J. A. (2006). The Effect of Varying Levels of Surfactant on the Reactive Uptake of N_2O_5 To Aqueous Aerosol. *Atmos. Chem. Phys.*, 6(6):1635–1644. doi:10.5194/acp-6-1635-2006.

Metcalf, A. R., Boyer, H. C., and Dutcher, C. S. (2016). Interfacial Tensions of Aged Organic Aerosol Particle Mimics Using a Biphasic Microfluidic Platform. *Environ. Sci. Technol.*, 50(3):1251–1259. doi:10.1021/acs.est.5b04880.

Mio, C., Gong, T., Terray, A., and Marr, D. W. M. (2000). Design of a Scanning Laser Optical Trap for Multiparticle Manipulation. *Rev. Sci. Instrum.*, 71(5):2196–2200. doi:10.1063/1.1150605.

Mitchem, L., and Reid, J. P. (2008). Optical Manipulation and Characterisation of Aerosol Particles Using a Single-Beam Gradient Force Optical Trap. *Chem. Soc. Rev.*, 37(4):756. doi:10.1039/b609713h.

Moon, H.-S., Nam, Y.-W., Park, J. C., and Jung, H.-I. (2009). Dielectrophoretic Separation of Airborne Microbes and Dust Particles Using a Microfluidic Channel for Real-Time Bioaerosol Monitoring. *Environ. Sci. Technol.*, 43(15):5857–5863. doi:10.1021/es900078z.

Morel, M., Galas, J.-C., Dahan, M., and Studer, V. (2012). Concentration Landscape Generators for Shear Free Dynamic Chemical Stimulation. *Lab Chip*, 12(7):1340–1346. doi:10.1039/C2LC20994B.

Nisisako, T., Torii, T., Takahashi, T., and Takizawa, Y. (2006). Synthesis of Monodisperse Bicolored Janus Particles with Electrical Anisotropy Using a Microfluidic Co-Flow System. *Adv. Mater.*, 18(9):1152–1156. doi:10.1002/adma.200502431.

Novosselov, I. V., Gorder, R. A., Van Amberg, J. A., and Ariessohn, P. C. (2014). Design and Performance of a Low-Cost Micro-Channel Aerosol Collector. *Aerosol Sci. Technol.*, 48(8):822–830. doi:10.1080/02786826.2014.932895.

Nozière, B. (2016). CLOUDS. Don't Forget the Surface. *Science*, 351(6280):1396–1397. doi:10.1126/science.aaf3253.

Okushima, S., Nisisako, T., Torii, T., and Higuchi, T. (2004). Controlled Production of Monodisperse Double Emulsions by Two-Step Droplet Breakup in Microfluidic Devices. *Langmuir*, 20(23):9905–9908. doi:10.1021/la0480336.

Olfert, J. S., Reavell, K. S., Rushton, M. G., and Collings, N. (2006). The Experimental Transfer Function of the Couette Centrifugal Particle Mass Analyzer. *J. Aerosol Sci.*, 37(12):1840–1852. doi:10.1016/j.jaerosci.2006.07.007.

Paprotny, I., Doering, F., Solomon, P. A., White, R. M., and Gundel, L. A. (2013). Microfabricated Air-Microfluidic

Sensor for Personal Monitoring of Airborne Particulate Matter: Design, Fabrication, and Experimental Results. *Sens. Actuators A Phys.*, 201:506–516. doi:10.1016/j.sna.2012.12.026.

Pathak, J. A., and Hudson, S. D. (2006). Rheo-Optics of Equilibrium Polymer Solutions: Wormlike Micelles in Elongational Flow in a Microfluidic Cross-Slot. *Macromolecules*, 39(25):8782–8792. doi:10.1021/ma061355r.

Petters, S. S., and Petters, M. D. (2016). Surfactant Effect on Cloud Condensation Nuclei for Two-Component Internally Mixed Aerosols. *J. Geophys. Res.*, 121(4):1878–1895. doi:10.1002/2015JD024090.

Phelan, F. R., Jr, Hudson, S. D., and Handler, M. D. (2005). Fluid Dynamics Analysis of Channel Flow Geometries for Materials Characterization in Microfluidic Devices. *Rheol. Acta.*, 45:59–71. doi:10.1007/s00397-005-0449-0.

Pilát, Z., Ježek, J., Kaňka, J., and Zemánek, P. (2014). Raman Tweezers in Microfluidic Systems for Analysis and Sorting of Living Cells. Edited by Daniel L Farkas, Dan V Nicolau, and Robert C Leif. *Proc. SPIE*, 8947:89471M. doi:10.1117/12.2040631.

Pope, F. D., Dennis-Smither, B. J., Griffiths, P. T., Clegg, S. L., and Cox, R. A. (2010). Studies of Single Aerosol Particles Containing Malonic Acid, Glutaric Acid, and Their Mixtures with Sodium Chloride. I. Hygroscopic Growth. *J. Phys. Chem. A*, 114(16):5335–5341. doi:10.1021/jp100059k.

Pöhlker, C., Wiedemann, K. T., Sinha, B., Shiraiwa, M., Gunthe, S. S., Smith, M., Su, H., Artaxo, P., Chen, Q., Cheng, Y., Elbert, W., Gilles, M. K., Kilcoyne, A. L. D., Moffet, R. C., Weigand, M., Martin, S. T., Pöschl, U., and Andreae, M. O. (2012). Biogenic Potassium Salt Particles as Seeds for Secondary Organic Aerosol in the Amazon. *Science*, 337(6098):1075–1078. doi:10.1126/science.1223264.

Prather, K. A., Bertram, T. H., Grassian, V. H., Deane, G. B., Stokes, M. D., DeMott, P. J., Aluwihare, L. I., Palenik, B. P., Azam, F., Seinfeld, J. H., Moffet, R. C., Molina, M. J., Cappa, C. D., Geiger, F. M., Roberts, G. C., Russell, L. M., Ault, A. P., Baltrusaitis, J., Collins, D. B., Corrigan, C. E., Cuadra-Rodriguez, L. A., Ebben, C. J., Forestieri, S. D., Guasco, T. L., Hersey, S. P., Kim, M. J., Lambert, W. F., Modini, R. L., Mui, W., Pedler, B. E., Ruppel, M. J., Ryder, O. S., Schoepp, N. G., Sullivan, R. C., and Zhao, D. (2013). Bringing the Ocean Into the Laboratory to Probe the Chemical Complexity of Sea Spray Aerosol. *Proc. Natl. Acad. Sci. U. S. A.*, 110(19):7550–7555. doi:10.1073/pnas.1300262110.

Pruppacher, H. R., and Klett, J. D. (2004). *Microphysics of Clouds and Precipitation*. 2nd ed. Kluwer Academic Publishers, New York.

Purcell, E. M. (1977). Life at Low Reynolds Number. *Am. J. Phys.*, 45(1):3–11. doi:10.1119/1.10903.

Quevedo, E., Steinbacher, J., and McQuade, D. T. (2005). Interfacial Polymerization Within a Simplified Microfluidic Device: Capturing Capsules. *J. Am. Chem. Soc.*, 127(30):10498–10499. doi:10.1021/ja0529945.

Rahman, N., Ibrahim, F., and Yafouz, B. (2017). Dielectrophoresis for Biomedical Sciences Applications: a Review. *Sensors*, 17(3):449–27. doi:10.3390/s17030449.

Reicher, N., Segev, L., and Rudich, Y. (2017). The WeIzmann Supercooled Droplets Observation (WISDOM) on a Microarray and Application for Ambient Dust. *Atmos. Meas. Tech. Discuss.*, [in review]. doi:10.5194/amt-2017-172.

Reid, J. P., Dennis-Smither, B. J., Kwamena, N.-O. A., Miles, R. E. H., Hanford, K. L., and Homer, C. J. (2011). The Morphology of Aerosol Particles Consisting of Hydrophobic and Hydrophilic Phases: Hydrocarbons, Alcohols and Fatty Acids as the Hydrophobic Component. *Phys. Chem. Chem. Phys.*, 13(34):15559–15572. doi:10.1039/c1cp21510h.

Riechers, B., Wittbracht, F., Huetten, A., and Koop, T. (2013). The Homogeneous Ice Nucleation Rate of Water Droplets Produced in a Microfluidic Device and the Role of Temperature Uncertainty. *Phys. Chem. Chem. Phys.*, 15(16):5873–5887. doi:10.1039/c3cp42437e.

Ruehl, C. R., Davies, J. F., and Wilson, K. R. (2016). An Interfacial Mechanism for Cloud Droplet Formation on Organic Aerosols. *Science*, 351(6280):1447–1450. doi:10.1126/science.aad4889.

Saarnio, K., Teinila, K., Saarikoski, S., Carbone, S., Gilardoni, S., Timonen, H., Aurela, M., and Hillamo, R. (2013). Online Determination of Levoglucosan in Ambient Aerosols with Particle-Into-Liquid Sampler &Ndash; High-Performance Anion-Exchange Chromatography &Ndash; Mass Spectrometry (PILS–HPAEC–MS). *Atmos. Meas. Tech.*, 6(10):2839–2849. doi:10.5194/amt-6-2839-2013.

Sackmann, E. K., Fulton, A. L., and Beebe, D. J. (2014). The Present and Future Role of Microfluidics in Biomedical Research. *Nature*, 507(7491):181–189. doi:10.1038/nature13118.

Sareen, N., Schwier, A. N., Shapiro, E. L., Mitroo, D., and McNeill, V. F. (2010). Secondary Organic Material Formed by Methylglyoxal in Aqueous Aerosol Mimics. *Atmos. Chem. Phys.*, 10(3):997–1016. doi:10.5194/acp-10-997-2010.

Schwier, A. N., Mitroo, D., and McNeill, V. F. (2012). Surface Tension Depression by Low-Solubility Organic Material in Aqueous Aerosol Mimics. *Atmos. Environ.*, 54(0):490–495. doi:10.1016/j.atmosenv.2012.02.032.

Schwier, A. N., Sareen, N., Mitroo, D., Shapiro, E. L., and McNeill, V. F. (2010). Glyoxal-Methylglyoxal Cross-Reactions in Secondary Organic Aerosol Formation. *Environ. Sci. Technol.*, 44(16):6174–6182. doi:10.1021/es101225q.

Schwier, A. N., Viglione, G. A., Li, Z., and Faye McNeill, V. (2013). Modeling the Surface Tension of Complex, Reactive Organic–Inorganic Mixtures. *Atmos. Chem. Phys.*, 13(21):10721–10732. doi:10.5194/acp-13-10721-2013.

Seinfeld, J. H., and Pandis, S. N. (2016). *Atmospheric Chemistry and Physics: From Air Pollution to Climate Change*. 3rd ed. John Wiley & Sons, Inc, New York.

Seo, M., Paquet, C., Nie, Z., Xu, S., and Kumacheva, E. (2007). Microfluidic Consecutive Flow-Focusing Droplet Generators. *Soft Matter*, 3(8):986–987. doi:10.1039/b700687j.

Shah, R. K., Shum, H. C., Rowat, A. C., Lee, D., Agresti, J. J., Utada, A. S., Chu, L.-Y., Kim, J.-W., Fernández-Nieves, A., Martinez, C. J., and Weitz, D. A. (2008). Designer Emulsions Using Microfluidics. *Mater. Today*, 11(4):18–27. doi:10.1016/S1369-7021(08)70053-1.

Shamloo, A., and Amirifar, L. (2016). A Microfluidic Device for 2D to 3D and 3D to 3D Cell Navigation. *J. Micromech. Microeng.*, 26(1). doi:10.1088/0960-1317/26/1/015003.

Shapiro, E. L., Szprengiel, J., Sareen, N., Jen, C. N., Giordano, M. R., and McNeill, V. F. (2009). Light-Absorbing Secondary Organic Material Formed by Glyoxal in Aqueous

Aerosol Mimics. *Atmos. Chem. Phys.*, 9(7):2289–2300. doi:10.5194/acp-9-2289-2009.

Shenoy, A., Rao, C. V., and Schroeder, C. M. (2016). Stokes Trap for Multiplexed Particle Manipulation and Assembly Using Fluidics. *Proc. Natl. Acad. Sci. U. S. A.*, 113 (15):3976–3981. doi:10.1073/pnas.1525162113.

Shields, C. W., IV, Reyes, C. D., and López, G. P. (2015). Microfluidic Cell Sorting: a Review of the Advances in the Separation of Cells From Debulking to Rare Cell Isolation. *Lab Chip*, 15(5):1230–1249. doi:10.1039/C4LC01246A.

Shih, S. C. C., Yang, H., Jebrail, M. J., Fobel, R., McIntosh, N., Al-Dirbashi, O. Y., Chakraborty, P., and Wheeler, A. R. (2012). Dried Blood Spot Analysis by Digital Microfluidics Coupled to Nanoelectrospray Ionization Mass Spectrometry. *Anal. Chem.*, 84(8):3731–3738. doi:10.1021/ac300305s.

Shulman, M. L., Jacobson, M. C., Carlson, R. J., Synovec, R. E., and Young, T. E. (1996). Dissolution Behavior and Surface Tension Effects of Organic Compounds in Nucleating Cloud Droplets. *Geophys. Res. Lett.*, 23(3):277–280. doi:10.1029/95GL03810.

Song, H., Chen, D. L., and Ismagilov, R. F. (2006). Reactions in Droplets in Microfluidic Channels. *Angew. Chem., Int. Ed.*, 45(44):7336–7356. doi:10.1002/anie.200601554.

Song, H., Tice, J. D., and Ismagilov, R. F. (2003). A Microfluidic System for Controlling Reaction Networks in Time. *Angew. Chem.*, 115(7):792–796. doi:10.1002/ange.200390172.

Song, M., Marcolli, C., Krieger, U. K., Lienhard, D. M., and Peter, T. (2013). Morphologies of Mixed Organic/Inorganic/Aqueous Aerosol Droplets. *Faraday Discuss.*, 165:289–316. doi:10.1039/c3fd00049d.

Sorooshian, A., Brechtel, F. J., Ma, Y., Weber, R. J., Corless, A., Flagan, R. C., and Seinfeld, J. H. (2006). Modeling and Characterization of a Particle-Into-Liquid Sampler (PILS). *Aerosol Sci. Technol.*, 40(6):396–409. doi:10.1080/02786820600632282.

Squires, T. M., and Quake, S. R. (2005). Microfluidics: Fluid Physics at the Nanoliter Scale. *Rev. Mod. Phys.*, 77(3):977–1026. doi:10.1103/RevModPhys.77.977.

Stan, C. A., Schneider, G. F., Shevkoplyas, S. S., Hashimoto, M., Ibanescu, M., Wiley, B. J., and Whitesides, G. M. (2009). A Microfluidic Apparatus for the Study of Ice Nucleation in Supercooled Water Drops. *Lab Chip*, 9(16):2293–2305. doi:10.1039/B906198C.

Steinbacher, J. L., and McQuade, D. T. (2006). Polymer Chemistry in Flow: New Polymers, Beads, Capsules, and Fibers. *J. Polym. Sci. A Polym. Chem.*, 44(22):6505–6533. doi:10.1002/pola.21630.

Steiner, B., Berge, B., Rühl, E., Rohmann, J., and Gausmann, R. (1999). Fast *In Situ* Sizing Technique for Single Levitated Liquid Aerosols. *Appl. Opt.*, 38(9):1523–1529. doi:10.1364/AO.38.001523.

Stone, H. A., Stroock, A. D., and Ajdari, A. (2004). Engineering Flows in Small Devices: Microfluidics Toward a Lab-on-a-Chip. *Annu. Rev. Fluid Mech.*, 36(1):381–411. doi:10.1146/annurev.fluid.36.050802.122124.

Sugiura, S., Nakajima, M., and Seki, M. (2002). Preparation of Monodispersed Polymeric Microspheres Over 50 Mm Employing Microchannel Emulsification. *Ind. Eng. Chem. Res.*, 41(16):4043–4047. doi:10.1021/ie0201415.

Sugiura, S., Nakajima, M., Itou, H., and Seki, M. (2001a). Synthesis of Polymeric Microspheres with Narrow Size Distributions Employing Microchannel Emulsification. *Macromol. Rapid Commun.*, 22(10):773–778. doi:10.1002/1521-3927(20010701)22:10<773::AID-MARC773>3.0.CO;2-H.

Sugiura, S., Nakajima, M., Iwamoto, S., and Seki, M. (2001b). Interfacial Tension Driven Monodispersed Droplet Formation From Microfabricated Channel Array. *Langmuir*, 17 (18):5562–5566. doi:10.1021/la010342y.

Sullivan, A. P., Weber, R. J., Clements, A. L., Turner, J. R., Bae, M. S., and Schauer, J. J. (2004). A Method for on-Line Measurement of Water-Soluble Organic Carbon in Ambient Aerosol Particles: Results From an Urban Site. *Geophys. Res. Lett.*, 31(13):L13105. doi:10.1029/2004GL019681.

Takayama, S., Ostuni, E., LeDuc, P., Naruse, K., Ingber, D. E., and Whitesides, G. M. (2001). Subcellular Positioning of Small Molecules. *Nature*, 411(6841):1016–1016. doi:10.1038/35082637.

Takeuchi, S., Garstecki, P., Weibel, D. B., and Whitesides, G. M. (2005). An Axisymmetric Flow—Focusing Microfluidic Device. *Adv. Mater.*, 17(8):1067–1072. doi:10.1002/adma.200401738.

Tanyeri, M., and Schroeder, C. M. (2013). Manipulation and Confinement of Single Particles Using Fluid Flow. *Nano Lett.*, 13(6):2357–2364. doi:10.1021/nl4008437.

Tanyeri, M., Ranka, M., Sittipolkul, N., and Schroeder, C. M. (2011). A Microfluidic-Based Hydrodynamic Trap: Design and Implementation. *Lab Chip*, 11(10):1786–1794. doi:10.1039/c0lc00709a.

Taylor, G. I. (1934). The Formation of Emulsions in Definable Fields of Flow. *Proc. R. Soc. London, Ser. A*, 146(858):501–523. doi:10.1098/rspa.1934.0169.

Thiele, J., Windbergs, M., Abate, A. R., Trebbin, M., Shum, H. C., Förster, S., and Weitz, D. A. (2011). Early Development Drug Formulation on a Chip: Fabrication of Nanoparticles Using a Microfluidic Spray Dryer. *Lab Chip*, 11(14):2362. doi:10.1039/c1lc20298g.

Tice, J. D., Song, H., Lyon, A. D., and Ismagilov, R. F. (2003). Formation of Droplets and Mixing in Multiphase Microfluidics at Low Values of the Reynolds and the Capillary Numbers. *Langmuir*, 19(22):9127–9133. doi:10.1021/la030090w.

Ting, T. H., Yap, Y. F., Nguyen, N.-T., Wong, T. N., Chai, J. C. K., and Yobas, L. (2006). Thermally Mediated Breakup of Drops in Microchannels. *Appl. Phys. Lett.*, 89(23):234101. doi:10.1063/1.2400200.

Toh, A. G. G., Wang, Z. P., Yang, C., and Nguyen, N.-T. (2014). Engineering Microfluidic Concentration Gradient Generators for Biological Applications. *Microfluid Nanofluid*, 16(1,2):1–18. doi:10.1007/s10404-013-1236-3.

Torza, S., and Mason, S. G. (1970). Three-Phase Interactions in Shear and Electrical Fields. *J. Colloid Interface Sci.*, 33 (1):67–83. doi:10.1016/0021-9797(70)90073-1.

Trinh, E. H. (1985). Compact Acoustic Levitation Device for Studies in Fluid Dynamics and Material Science in the Laboratory and Microgravity. *Rev. Sci. Instrum.*, 56(11):2059–2065. doi:10.1063/1.1138419.

Tsai, C.-J., and Pui, D. Y. H. (1990). Numerical Study of Particle Deposition in Bends of a Circular Cross-Section-Laminar Flow Regime. *Aerosol Sci. Technol.*, 12(4):813–831. doi:10.1080/02786829008959395.

Ulmke, H., Wriedt, T., and Bauckhage, K. (2001). Piezoelectric Droplet Generator for the Calibration of Particle-Sizing Instruments. *Chem. Eng. Technol.*, 24 (3):265–268. doi:10.1002/1521-4125(200103)24:3<265::AID-CEAT265>3.0.CO;2-4.

Unger, M. A., Chou, H.-P., Thorsen, T., Scherer, A., and Quake, S. R. (2000). Monolithic Microfabricated Valves and Pumps by Multilayer Soft Lithography. *Science*, 288 (5463):113–116. doi:10.1126/science.288.5463.113.

Utada, A. S., Chu, L.-Y., Fernández-Nieves, A., Link, D. R., Holtze, C., and Weitz, D. A. (2007). Dripping, Jetting, Drops, and Wetting: the Magic of Microfluidics. *MRS Bull.*, 32(09):702–708. doi:10.1557/mrs2007.145.

Utada, A. S., Lorenceau, E., Link, D. R., Kaplan, P. D., Stone, H. A., and Weitz, D. A. (2005). Monodisperse Double Emulsions Generated From a Microcapillary Device. *Science*, 308 (5721):537–541. doi:10.1126/science.1109164.

Vaughn, B. S., Tracey, P. J., and Trevitt, A. J. (2016). Drop-on-Demand Microdroplet Generation: a Very Stable Platform for Single-Droplet Experimentation. *RSC Adv.*, 6 (65):60215–60222. doi:10.1039/C6RA08472A.

Virtanen, A., Joutsensaari, J., Koop, T., Kannosto, J., Yli-Pirilä, P., Leskinen, J., Mäkelä, J. M., Holopainen, J. K., Pöschl, U., Kulmala, M., Worsnop, D. R., and Laaksonen, A. (2010). An Amorphous Solid State of Biogenic Secondary Organic Aerosol Particles. *Nature*, 467(7317):824–827. doi:10.1038/nature09455.

Wan, J., Bick, A., Sullivan, M., and Stone, H. A. (2008). Controllable Microfluidic Production of Microbubbles in Water−in−Oil Emulsions and the Formation of Porous Microparticles. *Adv. Mater.*, 20(17):3314–3318. doi:10.1002/adma.200800628.

Warschat, C., and Riedel, J. (2017). Studying the Field Induced Breakup of Acoustically Levitated Drops. *Rev. Sci. Instrum.*, 88(10):105108. doi:10.1063/1.5004046.

Weber, R. J., Orsini, D., Daun, Y., Lee, Y. N., Klotz, P. J., and Brechtel, F. (2001). A Particle-Into-Liquid Collector for Rapid Measurement of Aerosol Bulk Chemical Composition. *Aerosol Sci. Technol.*, 35(3):718–727. doi:10.1080/02786820152546761.

Welters, W., and Fokkink, L. (1998). Fast Electrically Switchable Capillary Effects. *Langmuir*, 14(7):1535–1538. doi:10.1021/la971153b.

Whitesides, G. M. (2006). The Origins and the Future of Microfluidics. *Nature*, 442(7101):368–373. doi:10.1038/nature05058.

Xu, S., Nie, Z., Seo, M., Lewis, P., Kumacheva, E., Stone, H. A., Garstecki, P., Weibel, D. B., Gitlin, I., and Whitesides, G. M. (2005). Generation of Monodisperse Particles by Using Microfluidics: Control Over Size, Shape, and Composition. *Angew. Chem., Int. Ed.*, 44(5):724–728. doi:10.1002/anie.200462226.

You, Y., Renbaum-Wolff, L., Carreras-Sospedra, M., Hanna, S. J., Hiranuma, N., Kamal, S., Smith, M. L., Zhang, X., Weber, R. J., Shilling, J. E., Dabdub, D., Martin, S. T., and Bertram, A. K. (2012). Images Reveal That Atmospheric Particles Can Undergo Liquid–Liquid Phase Separations. *Proc. Natl. Acad. Sci. U. S. A.*, 109(33):13188–13193. doi:10.1073/pnas.1206414109.

Zhang, S.-H., Akutsu, Y., Russell, L. M., Flagan, R. C., and Seinfeld, J. H. (1995). Radial Differential Mobility Analyzer. *Aerosol Sci. Technol.*, 23(3):357–372. doi:10.1080/02786829508965320.

Zhang, Y., Xiao, R.-R., Yin, T., Zou, W., Tang, Y., Ding, J., and Yang, J. (2015). Generation of Gradients on a Microfluidic Device: Toward a High-Throughput Investigation of Spermatozoa Chemotaxis. Edited by Chris D Wood. *PloS One*, 10(11). doi:10.1371/journal.pone.0142555.

Zhang, Z., Lin, Y. H., Zhang, H., Surratt, J. D., Ball, L. M., and Gold, A. (2012). Technical Note: Synthesis of Isoprene Atmospheric Oxidation Products: Isomeric Epoxydiols and the Rearrangement Products *Cis*- And *Trans*-3-Methyl-3,4-Dihydroxytetrahydrofuran. *Atmos. Chem. Phys.*, 12 (18):8529–8535. doi:10.5194/acp-12-8529-2012.

Zhao, Y., Chen, G., and Yuan, Q. (2006). Liquid−Liquid Two−Phase Flow Patterns in a Rectangular Microchannel. *AIChE J.*, 52(12):4052–4060. doi:10.1002/aic.11029.

Zhu, J., and Xuan, X. (2009). Particle Electrophoresis and Dielectrophoresis in Curved Microchannels. *J. Colloid Interface Sci.*, 340(2):285–290. doi:10.1016/j.jcis.2009.08.031.